

# Coding on Flag Manifolds for Limited Feedback MIMO Systems

---

Renaud-Alexandre Pitaval



# Coding on Flag Manifolds for Limited Feedback MIMO Systems

**Renaud-Alexandre Pitaval**

A doctoral dissertation completed for the degree of Doctor of Science in Technology to be defended, with the permission of the Aalto University School of Electrical Engineering, at a public examination held at the lecture hall S1 of the school on 31 January 2014 at 12 noon.

**Aalto University**  
**School of Electrical Engineering**  
**Department of Communications and Networking**

**Supervising professor**

Prof. Olav Tirkkonen

**Thesis advisor**

Prof. Olav Tirkkonen

**Preliminary examiners**

Prof. David J. Love, Purdue University, USA

Dos. Jyrki Lahtonen, University of Turku, Finland

**Opponent**

Prof. Robert Calderbank, Duke University, USA

Aalto University publication series

**DOCTORAL DISSERTATIONS** 211/2013

© Renaud-Alexandre Pitaval

ISBN 978-952-60-5491-9

ISBN 978-952-60-5492-6 (pdf)

ISSN-L 1799-4934

ISSN 1799-4934 (printed)

ISSN 1799-4942 (pdf)

<http://urn.fi/URN:ISBN:978-952-60-5492-6>

Unigrafia Oy

Helsinki 2013

Finland



**Author**

Renaud-Alexandre Pitaval

**Name of the doctoral dissertation**

Coding on Flag Manifolds for Limited Feedback MIMO Systems

**Publisher** School of Electrical Engineering**Unit** Department of Communications and Networking**Series** Aalto University publication series DOCTORAL DISSERTATIONS 211/2013**Field of research** Information Theory**Manuscript submitted** 14 June 2013**Date of the defence** 31 January 2014**Permission to publish granted (date)** 2 September 2013**Language** English **Monograph** **Article dissertation (summary + original articles)****Abstract**

The efficiency of the physical layer in modern communication systems using multi-input multi-output (MIMO) techniques is largely based on the availability of channel state information (CSI) at the transmitter. In many practical systems, CSI needs to be quantized at the receiver side before transmission through a limited rate feedback channel. This is typically done using a codebook-based precoding transmission, where the receiver transmits the index of a codeword from a pre-designed codebook shared with the transmitter. To construct such codes one has to discretize complex flag manifolds. For single-user MIMO with a maximum likelihood receiver, the spaces of interest are Grassmann manifolds. With a linear receiver and network MIMO, the codebook design is related to discretization of Stiefel manifolds and more general flag manifolds.

In this thesis, coding in flag manifolds is studied. In a first part, flag manifolds are defined as metric spaces corresponding to subsurfaces of hyperspheres. The choice of distance defines the geometry of the space and impacts clustering and averaging (centroid computation) in vector quantization, as well as coding theoretical packing bounds and optimum constructions.

For two transmitter antenna systems, the problem reduces to designing spherical codes. A simple isomorphism enables to analytically derive closed-form codebooks with inherent low-implementation complexity. For more antennas, the concept of orbits of symmetry groups is investigated. Optimum codebooks, having desirable implementation properties as described in industry standardization, can be obtained using orbits of specific groups.

For large antenna systems and base station cooperation, a product codebook strategy is also considered. Such a design requires to jointly discretize the Grassmann and Stiefel manifolds. A vector quantization algorithm for joint Grassmann-Stiefel quantization is proposed. Finally, the pertinence of flag codebook design is illustrated for a MIMO system with linear receiver.

**Keywords** MIMO systems; quantization; coding; flag, Stiefel, Grassmann, manifolds**ISBN (printed)** 978-952-60-5491-9**ISBN (pdf)** 978-952-60-5492-6**ISSN-L** 1799-4934**ISSN (printed)** 1799-4934**ISSN (pdf)** 1799-4942**Location of publisher** Helsinki**Location of printing** Helsinki**Year** 2013**Pages** 161**urn** <http://urn.fi/URN:ISBN:978-952-60-5492-6>



# Preface

The research work for this doctoral thesis has been carried out at the department of Communications and Networking of Aalto University. The work was funded by the Finnish Funding Agency for Technology and Innovation, the Academy of Finland, Nokia Foundation, and HPY Foundation.

First and foremost, I wish to express my gratitude to my supervisor Prof. Olav Tirkkonen for his support and guidance. Working with Prof. Tirkkonen was a great pleasure and a continuous journey of learning through many enlightening discussions.

Part of this work was also done at the Image Processing and Communications Laboratory, Queen's University, Canada, during 2009-2010. I would like to sincerely thank Prof. Steven D. Blostein for his kindness and support during my stay at Queen's. I wish also to thank Lect. Wei Dai for welcoming me in his group at Imperial College London for a research visit in Spring 2013.

I am thankful to the co-authors of the papers included in this thesis, Karol Schober, Prof. Risto Wichman, and Ashivin Srinivasan, and especially Dr. Helka Määttänen for valuable instructions when I started at the department. I would like also to thank the thesis preliminary examiners, Prof. David J. Love and Dos. Jyrki Lahtonen, for their constructive comments; and Prof. Robert Calderbank for accepting to be the defence opponent.

I am grateful to all nice friends and colleagues I have met during these past years in Finland, Canada, and UK. Mes remerciements les plus sincères sont destinés à ma chère et tendre épouse, Viet-Anh, pour son amour, son soutien, et son illustration plein d'humour de ce manuscrit.

Helsinki, November 28, 2013,

Renaud-Alexandre Pitaval



# Contents

<b>Preface</b>	<b>i</b>
<b>Contents</b>	<b>iii</b>
<b>List of Publications</b>	<b>v</b>
<b>1. Introduction</b>	<b>1</b>
1.1 Background . . . . .	1
1.2 Objective and Scope . . . . .	3
1.3 Contribution and Structure of the Thesis . . . . .	3
1.4 Summary of Publications . . . . .	5
<b>2. System Model</b>	<b>9</b>
2.1 Signal and Channel Model . . . . .	9
2.2 Base Station Cooperation . . . . .	10
2.3 Codebook-Based Precoding . . . . .	11
2.4 Low-Complexity Constraints . . . . .	11
<b>3. Flag Manifolds: Code Designs and Geometry</b>	<b>13</b>
3.1 Flag Manifolds . . . . .	13
3.2 Spherical Embeddings and Chordal Distances . . . . .	15
3.3 Codebook Designs . . . . .	16
3.4 Lloyd's Algorithm and Centroids . . . . .	17
3.5 Density and Packing Bounds . . . . .	18
<b>4. Grassmannian Pakings for 2-Tx MIMO</b>	<b>23</b>
4.1 Grassmannian Codebooks from Spherical Arrangements . .	23
4.2 Low Implementation-Complexity Codes . . . . .	26
4.3 Quantization Error Analysis . . . . .	28
<b>5. Flag and Stiefel Orbit Codes</b>	<b>31</b>



5.1	Orbits of Projective Group Representations . . . . .	31
5.2	Extraspecial Group Code Constructions . . . . .	35
5.3	Expansion to Stiefel Codes . . . . .	38
<b>6.</b>	<b>Joint Grassmann-Stiefel Codes for Product Codebooks</b>	<b>41</b>
6.1	Product Codebook-Based Precoding . . . . .	41
6.2	Joint Grassmann-Stiefel Codebooks . . . . .	43
6.3	Lloyd-type Algorithm for Joint Grassmann-Stiefel Codebook	46
6.4	Codeword Selections . . . . .	47
<b>7.</b>	<b>Flag Codebooks for MIMO Systems with Linear Receiver</b>	<b>51</b>
7.1	Achievable Information Rates . . . . .	52
7.2	Linear Receiver versus ML Receiver . . . . .	52
7.3	Codebook Designs . . . . .	53
7.4	Simulations . . . . .	54
<b>8.</b>	<b>Conclusions</b>	<b>57</b>
	<b>Bibliography</b>	<b>61</b>
	<b>Errata</b>	<b>67</b>
	<b>Publications</b>	<b>71</b>

# List of Publications

This thesis consists of an overview and of the following publications which are referred to in the text by their Roman numerals.

- I** R.-A. Pitaval, O. Tirkkonen and S. D. Blostein. Density and Bounds for Grassmannian Codes with Chordal Distance. In *Proceedings of the IEEE International Symposium on Information Theory (ISIT)*, Saint Petersburg, Russia, pp. 2298-2302, Aug. 2011.
- II** R.-A. Pitaval and O. Tirkkonen. Volume of Ball and Hamming-type Bounds for Stiefel Manifold with Euclidean Distance. In *Proceedings of the 46th Annual Asilomar Conference on Signals, Systems, and Computers (ACSSC)*, Pacific Grove, California, pp. 483-487, Nov. 2012.
- III** R.-A. Pitaval, H.-L. Määttänen, K. Schober, O. Tirkkonen, and R. Wichman. Beamforming Codebooks for Two Transmit Antenna Systems based on Optimum Grassmannian Packings. *IEEE Transactions on Information Theory*, vol.57, no.10, pp. 6591-6602, Oct. 2011.
- IV** R.-A. Pitaval, O. Tirkkonen and S. D. Blostein. Low Complexity MIMO Precoding Codebooks from Orthoplex Packings. In *Proceedings of the IEEE International Conference on Communications (ICC)*, Kyoto, Japan, pp. 1-5, June 2011.
- V** R.-A. Pitaval and O. Tirkkonen. Grassmannian Packings from Orbits of Projective Group Representations. In *Proceedings of the 46th Annual Asilomar Conference on Signals, Systems, and Computers (ACSSC)*, Pa-

cific Grove, California, pp. 478-482, Nov. 2012.

**VI** R.-A. Pitaval and O. Tirkkonen. Flag Orbit Codes and Their Expansion to Stiefel Codes. In *Proceedings of the IEEE Information Theory Workshop (ITW)*, Seville, Spain, pp. 360-364, Sep. 2013.

**VII** R.-A. Pitaval and O. Tirkkonen. Joint Grassmann-Stiefel Quantization for MIMO Product Codebooks. Accepted for publication in *IEEE Transactions on Wireless Communications*, 13 pp., Oct. 2013.

**VIII** R.-A. Pitaval, A. Srinivasan and O. Tirkkonen. Codebooks in Flag Manifolds for Limited Feedback MIMO Precoding. In *Proceedings of the 9th International ITG Conference on Systems, Communications and Coding (SCC)*, Munich, Germany, pp. 1-5, Jan. 2013.

### **Author's Contribution**

The author has had a leading role in writing all the publications. The author has had a leading role in the planning and the analysis of Publications [I, II, IV, VII]. The author has participated in theoretical modeling and design of experiments in Publications [III, V, VI, VIII]. The author has conducted the performance simulations for all publications except Publication VIII.

# List of abbreviations and symbols

## Abbreviations

2D	two dimension
3D	three dimension
4D	four dimension
4G	4 <sup>th</sup> generation systems
BS	base station
CB	codebook
CoMP	coordinated multi-points
CSI	channel state information
dB	decibel
EP	Equal transmit-power per-antenna
FDD	frequency-division duplexing
HB	Hamming bound
i.i.d	independent and identically distributed
LTE	long-term evolution
MIMO	multiple-input multiple-output
ML	maximum likelihood
MMSE	minimum mean square error
MS-MUB	maximal set of mutually unbiased bases
MU	multi-user
MUB	mutually unbiased bases
pdf	probability density function
SISO	single-input single-output
SNR	signal-to-noise ratio
SU	single-user
Rx	receive antenna
ZF	zero forcing

**Symbols**

$\mathbb{C}$	complex field
$\mathbb{CP}^1$	complex projective line
$\mathcal{C}$	codebook
$\mathcal{C}_k$	border of the $k^{\text{th}}$ spherical cap
$\mathbf{c}_k$	$k^{\text{th}}$ spherical codeword
$\mathbf{C}_k$	$k^{\text{th}}$ codeword
$\mathcal{C}_{\text{pr}}$	product codebook
$d_c$	chordal distance
$d_f$	flag chordal distance
$d_g$	Grassmann chordal distance
$d_{\text{mu}}$	MUness flag distance
$d_p$	permutation-invariant flag chordal distance
$d_s$	Stiefel chordal distance
$D$	dimension of embedding sphere
$D_{\mathcal{M}}(\mathcal{C})$	average squared distortion of codebook $\mathcal{C}$ on manifold $\mathcal{M}$
$\mathbf{D}$	diagonal matrix
$\det$	determinant
$\mathbb{E}[\cdot]$	mathematical expectation
$\mathbf{F}$	part of linear receiver
$f_{d_g^2}$	pdf of squared Grassmann distortion
$\mathcal{F}_{n_t, s_1, \dots, s_r}^{\mathbb{C}}$	$n_t$ -by- $n_s$ complex flag manifold with equivalence under $r$ unitary groups of size $s_i$
$\vec{\mathcal{F}}_{n_t, s_1, \dots, s_r}^{\mathbb{C}}$	$n_t$ -by- $n_s$ complex flag manifold with equivalence under $r$ unitary groups of size $s_i$ and permutation of the $r$ groups of substreams
$\mathcal{F}_{n_t, n_s}^{\mathbb{C}}$	$n_t$ -by- $n_s$ complex flag manifold with equivalence under $n_s$ phase rotation
$\vec{\mathcal{F}}_{n_t, s_1, \dots, s_r}^{\mathbb{C}}$	$n_t$ -by- $n_s$ complex flag manifold with equivalence under $n_s$ phase rotation and permutation of the $n_s$ columns
$g$	an abstract group element
$G$	an abstract group
$\mathbf{G}$	large-scale path gain matrix
$\mathcal{G}_{n_t, n_s}^{\mathbb{C}}$	complex $n_t$ -by- $n_s$ Grassmann manifold
$\mathbf{H}$	fading channel
$\mathbf{H}_{\text{eff}}$	effective fading channel

$\mathbf{H}_k$	fading channel from $k^{\text{th}}$ BS
$\mathbf{H}_{\text{ls}}$	large-scale fading channel
$\mathbf{H}_{\text{ss}}$	small-scale fading channel
$\bar{I}$	average information rate
$I_{\text{lr}}$	information rate with linear receiver
$I_{\text{ml}}$	information rate with ML receiver
$I_{n_m}$	maximum achievable rate without transmission rank constraint
$I_{n_s}$	maximum achievable rate with $n_s$ streams
$\mathbf{I}_{n_t}$	$n_t$ -by- $n_t$ identity matrix
$\mathbf{I}_{n_t, n_s}$	$n_t$ -by- $n_s$ identity matrix
$K_b$	number of bits to represent a real number
$\log_2$	binary logarithm
$\mathcal{M}$	manifold
$\mathbf{n}$	noise vector
$n_{\text{bs}}$	number of BSs
$n_{\text{cb}}$	size of codebook
$n_r$	number of receive antennas
$n_s$	number of streams
$n_t$	number of transmit antennas
$N_g$	Grassmann codebook cardinality
$N_s$	Stiefel codebook cardinality
$\mathbf{P}$	permutation matrix
$\mathcal{PU}_{n_t}$	projective unitary group of size $n_t$
$\text{q}_C$	abstract quantization map associated with $C$
$\text{q}^*$	optimum quantization map using information rate
$\text{q}_c$	quantization map using chordal distance
$\text{q}_g$	quantization map using Grassmann chordal distance
$r$	number of subgroups of streams
$R$	radius of embedding sphere
$\mathcal{R}_k$	$k^{\text{th}}$ Voronoi cell
$\mathbb{R}$	real field
$s_k$	$k^{\text{th}}$ group of substreams
$S_r$	symmetric group of degree $r$
$S^D(R)$	$D$ -sphere of radius $R$
$\mathcal{SO}_{n_t}$	special orthogonal group of size $n_t$
$\mathfrak{u}(n_s)$	vector space of skew-Hermitian $n_s$ -by- $n_s$ matrices, Lie algebra for $\mathcal{U}_{n_s}$

$\mathcal{U}_{n_t}$	unitary group of size $n_t$
$\mathbf{U}$	unitary matrix
$\mathbf{U}_i$	unitary matrix of size $s_i$
$\mathcal{V}_{n_t, n_s}^{\mathbb{C}}$	complex $n_t$ -by- $n_s$ Stiefel manifold
$V$	random source on Stiefel manifold
$\mathbf{v}$	point on sphere
$\mathbf{v}_k$	$k^{\text{th}}$ column of $\mathbf{V}$
$\mathbf{V}$	$n_t$ -by- $n_s$ Stiefel matrix
$\mathbf{V}_k$	$n_t$ -by- $s_k$ Stiefel submatrix of $\mathbf{V}$
$\mathbf{V}_{\text{ls}}$	$n_s$ -largest right singular vectors of $\mathbf{W}_{\text{ls}}$
$\mathbf{V}_{\text{ss}}$	$n_s$ -largest right singular vectors of $\mathbf{W}_{\text{ss}}$
$\mathbf{w}$	precoding vector
$\mathbf{W}$	precoding matrix
$\mathbf{W}_{\text{ls}}$	large-scale precoder
$\mathbf{W}_{\text{ss}}$	small-scale precoder
$\mathbf{x}$	transmitted symbol vector
$\mathbf{y}$	received signal
$\mathbf{y}_k$	$k^{\text{th}}$ column of $\mathbf{Y}$
$\mathbf{Y}$	$n_t$ -by- $n_s$ Stiefel matrix
$\mathbf{Y}_k$	$n_t$ -by- $s_k$ Stiefel submatrix of $\mathbf{Y}$
$Z(G)$	center of group $G$
$\mathbf{Z}_k$	centroid of $k^{\text{th}}$ Voronoi cell
$\alpha_k$	large-scale path gain from $k^{\text{th}}$ BS
$\delta_{\mathcal{M}}(\mathcal{C})$	minimum chordal distance of codebook $\mathcal{C}$ on manifold $\mathcal{M}$
$\delta_g$	minimum Grassmann chordal distance
$\delta_s$	minimum Stiefel chordal distance
$\gamma$	snr per-stream
$\gamma_k$	post-processing SINR of the $k^{\text{th}}$ data stream
$\lambda_k$	$k^{\text{th}}$ singular value of $\mathbf{H}_{\text{eff}}$
$\theta$	angle
$\phi$	angle
$\varphi$	angle
$\mu(B(r_n))$	normalized volume of a ball of radius $r_n$
$\sigma$	permutation
$\sigma_k$	$k^{\text{th}}$ singular value of $\mathbf{H}$
$\cdot^H$	Hermitian transpose

# 1. Introduction

## 1.1 Background

Multi-input multi-output (MIMO) techniques are key technologies to enhance spectrum efficiency of wireless systems. Performance heavily depends on the channel state information (CSI) available at the transmitter. MIMO using linear precoding have been shown to achieve large capacity gains over traditional single-input-single-output (SISO) systems [32, 87]. Linear precoding for single and multiple stream transmission, a.k.a. beamforming and multiple beamforming, has been intensely investigated for point-to-point communications [75, 89]. Without channel reciprocity, e.g. in frequency-division duplex systems, the only way to acquire CSI is through a limited feedback channel. Fortunately, few bits is usually enough to fill most of the gap between open-loop and closed-loop capacity [55]. A widely applied method is to use codebook-based precoding in which the receiver selects a precoding codeword from a predefined codebook and feeds back the index to the transmitter. Since it is more important to feed back the channel direction than the channel beam gain [23], the quantization of the channel is often done with a rectangular unitary code.

In point-to-point communications with maximum likelihood receiver, the performance of a unitary precoding codebook is related to its interpretation as a discretization of the Grassmann manifold [22, 23, 53, 55, 56, 61]. Codebook design criteria are based on extremization of average distortion metrics [22, 59, 63, 71, 72, 95]. The information rate is approximately a function of the distortion rate of the codebook associated with Grassmann chordal distance as a quantization map [22, 23]. In [56, 61] the beamforming codebook design problem for uncorrelated channel was linked to a



suboptimal approach, the Grassmannian line packing problem, i.e. maximizing the minimum distance of the codebook. Extension to correlated channel through codebook rotation is then provided in [54, 95].

Grassmann packing, originally a mathematical problem of independent interest [18], was thus retained as a method for codebook design. Extensive tables of real Grassmannian codes could be found in the literature [83]. For the complex Grassmannian, fewer results were available [15, 79, 85]. Complex Grassmann code construction was hence addressed in [24, 56, 64, 72, 76, 95, 96], codes being generated by computer searched by either directly minimizing the distortion of the codebook using vector quantization algorithms such as Lloyd-type algorithms [64, 72, 95]; or maximizing its minimum distance with brute-force search [56], modified Lloyd's algorithm [96], alternating projection algorithm [24], and expansion-compression algorithm [76]. Analytical constructions were presented in [2, 4–6, 96] with application also to non-coherent MIMO space-time coding [97], and low-complexity implementation codebooks for precoding [44, 51, 60].

While Grassmann precoding has attracted much attention, other transmission scenarios or constraints may lead to the need of designing codebooks in other spaces. Practical codebooks in industry standards have been designed according to power and implementation-complexity constraints [51]. With an MMSE or ZF receiver, the set of non-equivalent precoding matrices is not a Grassmann manifold anymore [57]. In [57], the proper space of quantization is presented along with some optimum analytical packings for 2 transmit antenna systems. For bit-interleaved multiple beamforming, it is shown in [77] that the optimum precoder is only invariant under a diagonal unitary transform, a corresponding Lloyd's algorithm is presented.

Further development of MIMO techniques towards network-level processing are expected to bring performance enhancements. In MIMO broadcasting, unitary codebook-based precoding has been well-investigated in a multi-user (MU) setting with one-stream transmission per-user [43, 47, 90, 91]. In [47], codebook design on a different Riemannian manifold than the Grassmann manifold is considered, and accordingly, a systematic construction of structured codebook is presented. While considering different system models, the manifolds discussed in [47] and [57] are the same, and the proposed distance metrics are equivalent up to a scaling factor. Similar equivalence classes are described in [90, 91]. To deal with the

specific features of base stations cooperation or coordinated multi-points (CoMP) [46, 48, 88], a product codebook quantization strategy was proposed in [16].

Interpreting all those designs in a unified manner, the spaces of discretization to consider are quotient spaces of unitary groups, and although not recognized as such, so-called *flag manifolds*. Literature on flag manifolds can be found in quantum theory context, e.g. in [62, 68, 98].

## 1.2 Objective and Scope

The goal of the thesis is to design low-implementation complexity precoding codebooks with analytic and algebraic methods. Finding optimal precoding codebooks is equivalent to the problem of discretizing a manifold. Manifold discretization is a generic mathematical problem covering for example the particular case of spherical arrangements or real Grassmannian discretization which have been addressed due to their relevance to many fields of science such as chemistry, biology and physics. While there is an increased interest in manifold discretization from communications engineers, there are few results from the mathematical literature. Analytical discretization of complex manifolds yields mathematically structured codebooks which are amenable for implementation. In this work, we concentrate on discretization techniques for quotient spaces of unitary groups, so-called flag manifolds, including Stiefel and Grassmann manifolds.

## 1.3 Contribution and Structure of the Thesis

This dissertation contributes to the field of coding theory for unitary manifolds and codebook design for MIMO precoding.

We address several codebook constructions in the literature as a unified mathematical problem of discretization of flag manifolds. The Conway-Hardin-Sloane spherical embedding of the Grassmann manifold with chordal distance is generalized to other flag manifolds, and modified for equal-power per-antenna codebooks. The spherical embeddings allow leveraging results from the mathematical literature. For Lloyd's algorithms, we leverage a result on centroid computation on Euclidean embedded surfaces applicable to manifolds equipped with a chordal distance. In par-

ticular, we derive a closed-form centroid computation in the Stiefel manifold. The spherical embeddings induce also coding bounds from the sphere packing literature.

A fundamental problem of coding theory is to establish the maximum cardinality of a code for a given distance. The well-known Hamming bound partially answers this question. We have investigated the density of packings in the complex Grassmann and Stiefel manifolds equipped with chordal distance. We have computed the exact volume of the Grassmann and Stiefel manifold induced by their chordal distance. This has application in the evaluation of the volume of a small metric ball which is critical to derive Hamming-type bounds. We provide a refinement of the Hamming bound for Grassmannian codes and a generalization of a bound on minimum distance previously proven only for line packings. This result is later generalized to all manifolds with a metric induced by an embedding in a Euclidean hypersphere. For these manifolds, of which the Stiefel manifold, this provides results generalizing previously known bounds on codes in the unitary group.

We then investigate explicit analytical code constructions, looking for codebooks having their entries in a limited set of complex numbers. For the special case of two antenna precoding codebooks, the  $2 \times 1$  complex Grassmannian is isometric to a real sphere, so that designing  $2 \times 1$  complex Grassmannian packing is equivalent to the real sphere packing problem. Based on the extensive literature on this topic, we have derived optimal closed-form codebooks using a simple isomorphism. Using the simple geometry of some of these codebooks, we also derived closed-form expression of the corresponding SNR gain due to beamforming. Additionally, we investigate codebooks based on other spherical arrangements, such as solutions maximizing the harmonic mean of the mutual distances among the codewords. We found that in most of cases, Grassmannian codebooks based on these other spherical arrangements outperform codebooks from Grassmannian packings. The reason is that the mean distance provides a better approximation of the average distortion than the minimal distance.

Next, to address the problem of manifold discretization in more general manner we use the concept of an orbit of a symmetry group. We generalize the concept of spherical orbit codes to flag orbit codes and derive basic properties. For flag codes, projective unitary representations of finite group are of specific interests. We consider some finite groups having appropriate representations and find appropriate initial points heuristically.

We give explicit codes in Grassmann and other simple flag manifolds in 2D and 4D. Using a construction related to representation theory, families of packings are obtained for any dimension of a power of a prime. We prove that some of these packings are optimal in relation with a power per-antenna constraint. We also investigate Stiefel orbit codes arising from the linear representation of the projective group considered. By doing so, one obtains expansions of the Grassmann orbit codes to the Stiefel manifold.

Then, we discuss codebook designs for two different transmission scenarios. For a base station cooperation system, we consider a product codebook strategy where a single small codebook is implemented at the receiver. We show that near optimal performance can be reached with an appropriate choice of Stiefel representatives of Grassmann codes. Accordingly, we propose a novel joint Grassmann-Stiefel codebook design aiming at good quantization of Grassmann and Stiefel manifolds with a single codebook. A Lloyd-type algorithm generating a Stiefel codebook conditioned on a fixed Grassmannian codebook is presented. Furthermore, concrete examples of analytical joint Grassmann-Stiefel packings are also given. We also discuss low-complexity suboptimal codeword selection methods.

Finally, the codebook design problem for MIMO with a linear receiver is related to a discretization problem of generalized flag manifolds. With a linear receiver, we show that the spaces of equivalent precoders are simple permutation-invariant flag manifolds. We describe a Lloyd-type algorithm for these spaces and compare the achievable rate with the generated codebooks by simulation. When the number of streams, and the number of receive and transmit antennas are the same, the simulations show that the marginal gain from precoding is relatively small with few feedback bits for more than two transmit antennas. This differs from low-rank transmission with optimum receivers, where a small number of feedback bits allows near-optimal channel adaptation.

## 1.4 Summary of Publications

This thesis consists of an introductory part and eight original publications.

The first two papers are discussing coding theoretical problems on the Grassmann and Stiefel manifolds.

In Publication I, the density of Grassmann codes with the chordal distance is investigated. From the observation that the kissing radius cannot be determined solely from the minimum distance, upper and lower bounds are provided, along with the corresponding bounds on the density. This leads to a refinement of the Hamming bound for Grassmannian codes. Finally, we provide explicit bounds on code cardinality and minimum distance, notably a generalization of a bound on minimum distance previously proven only for line packings.

In Publication II, the density of Stiefel codes is investigated. We compute the volume of the Stiefel manifold induced by the chordal distance. This has a direct application for evaluating the volume of a small metric ball critical to derive Hamming-type bounds. Using a spherical embedding argument, we provide results generalizing previously known bounds on codes in the Grassmann manifold and the unitary group.

The following four papers deal with explicit code constructions.

In Publication III, we construct Grassmann beamforming codebooks for two transmit antenna systems. Using an isometry, we show that the discretization problems are directly solved by corresponding spherical codes. Notably, the Grassmannian line packing problem is equivalent to the Tammes problem on the real sphere, so that optimum spherical packings give optimum Grassmannian packings. Moreover, a simple isomorphism enables to analytically derive simple codebooks in closed-form having low implementation complexity. Using the simple geometry of some of these codebooks, we derive closed-form expressions of the probability density function (pdf) of the squared quantization error. We also investigate codebooks based on other spherical arrangements, such as solutions maximizing the harmonic mean of the mutual distances among the codewords, which is known as the Thomson problem. We find that in most of the cases, Grassmannian codebooks based on these other spherical arrangements outperform codebooks from Grassmannian packing.

In Publication IV, a construction of Grassmannian packings related to representation theory is applied to build implementation-friendly MIMO precoding codebooks when the number of transmit antennas is a power of a prime number. Using chordal distance as a metric, some of the corresponding packings are optimal by meeting the orthoplex bound. In addition, by using only some of the codewords, smaller packings satisfying an equal-power per antenna constraint can be constructed. Optimality with reference to this constraint is shown by modifying Conway-Hardin-

Sloane's spherical embedding of the Grassmann manifold for equal-power per-antenna codebooks.

In Publications V and VI, we discuss group orbits to construct codes in Grassmann and flag manifolds, respectively.

In Publications V, to generate Grassmann orbit codes, we look for projective unitary representations of finite groups. Following this principle, we derive basic properties and describe explicit constructions of group orbits leading to some optimum packings in 2 and 4 dimensions.

In Publication VI, we define distances that embed flag manifolds into Euclidean hyperspheres, providing a generalization of the spherical embedding of Grassmann manifolds equipped with the so-called chordal distance. For code construction, the center of a finite unitary group has no effect, and thus it is sufficient to consider its inner automorphism group. Accordingly, some explicit constructions from projective unitary representations of finite groups in 2 and 4 dimensions are described. We also give examples of codes on the Stiefel manifold constructed as orbits of the linear representation of the projective groups, leading to codes that are expansions of the flag codes considered.

The last two papers investigate scenarios where Grassmann codebook design is not optimal, and a larger manifold has to be considered.

In Publication VII, we focus on product codebook design with application to cooperative MIMO transmission. We show that the Stiefel representatives which are used to realize a Grassmann codebook impact the performance of product codebooks. We propose a novel joint Grassmann-Stiefel codebook design aiming at good discretization of Grassmann and Stiefel manifolds with a single codebook. The resulting product codebooks show performance comparable with global Grassmann quantization. To find low-distortion codebooks, we present a vector quantizer to generate Stiefel codebooks conditioned on a fixed Grassmann codebook. For this purpose, we provide an exact solution for computing centroids in the Stiefel manifold with chordal distance. Furthermore, concrete examples of analytical joint Grassmann-Stiefel packings are given. Additionally, we discuss low-complexity codeword selection methods.

Publication VIII interpretes unitary codebook design problems for various precoded MIMO scenarios as generalized discretization problems of flag manifolds. As a concrete example, we consider codebooks for MIMO transmission with linear receivers. In this case, the problem reduces to discretizing permutation-invariant flag manifolds. A corresponding

Lloyd's algorithm is given, providing low-distortion codebooks. We found that a full-rank MIMO system with the same number of transmit and receive antennas, the gain of precoding with linear receiver is small. This differs from the behavior of low-rank transmissions, where it is known that a small number of feedback bits allows near-optimal channel adaptation.

## 2. System Model

This chapter presents the system model of codebook-based MIMO precoding [51, 55]. For point-to-point MIMO, we consider a uncorrelated flat Rayleigh MIMO channel. Extension to base station cooperation is modeled by integrating large-scale path gain imbalance between the transmitters, similarly than in [16]. The system model motivates the prime interest of the thesis which is on code design and construction.

### 2.1 Signal and Channel Model

Consider a MIMO system with  $n_t$  transmit and  $n_r$  receive antennas. After unitary precoding with  $\mathbf{W} \in \mathbb{C}^{n_t \times n_s}$ , a vector  $\mathbf{x} \in \mathbb{C}^{n_s \times 1}$  of  $n_s \leq \min(n_t, n_r)$  multiplexed streams is transmitted through a fading channel  $\mathbf{H} \in \mathbb{C}^{n_r \times n_t}$ . The received signal is

$$\mathbf{y} = \mathbf{H}\mathbf{W}\mathbf{x} + \mathbf{n}, \quad (2.1)$$

$$= \mathbf{H}_{\text{eff}}\mathbf{x} + \mathbf{n}, \quad (2.2)$$

$\mathbf{n} \in \mathbb{C}^{n_r \times 1}$  denote the noise, and  $\mathbf{H}_{\text{eff}} = \mathbf{H}\mathbf{W}$  the effective channel. We assume that the transmitted signal and the noise are Gaussian with covariances  $\mathbb{E}[\mathbf{x}\mathbf{x}^H] = \gamma\mathbf{I}_{n_s}$  and  $\mathbb{E}[\mathbf{n}\mathbf{n}^H] = \mathbf{I}_{n_r}$ , where  $\gamma$  is the per-stream SNR. We assume the entries of the channel  $\mathbf{H}$  are independent and identically distributed (i.i.d) complex normal variables with zero mean and unit variance.

We concentrate on the properties of  $\mathbf{W}$  related to steering the transmitted energy to the signal subspace of the receiver and increasing the capacity. Here, power allocation is considered to be out of scope of precoding and instead form a part of the design of  $\mathbf{x}$ . We thus have the following constraints on  $\mathbf{W}$ : the total transmit power is  $n_s$ , which is equally shared among the symbols such that  $\mathbf{W}^H\mathbf{W} = \mathbf{I}_{n_s}$ . The precoder, which is a func-



tion of the received feedback bits, is used for channel adaptation in order to increase to maximum achievable information rate of the system given by

$$\bar{I} = \mathbb{E} [\log_2 \det (\mathbf{I} + \gamma \mathbf{H}_{\text{eff}}^H \mathbf{H}_{\text{eff}})]. \quad (2.3)$$

## 2.2 Base Station Cooperation

In Chapter 6, we consider cooperative transmission from several base stations to the same user. Then, we define a  $(n_{bs} \times n_t) \times n_s$  MIMO system as  $n_{bs}$  base stations (BSs) each equipped with  $n_t$  antennas transmitting cooperatively  $n_s$ -data streams. It is assumed that the BSs are able to instantaneously share the feedback information, e.g. via high speed back-hauls. The effective channel becomes

$$\mathbf{H}_{\text{eff}} = \mathbf{H}_{\text{ls}} \mathbf{W}_{\text{ls}}, \quad (2.4)$$

where  $\mathbf{W}_{\text{ls}}$  is an  $n_{bs}n_t \times n_s$  aggregate precoding matrix and

$$\mathbf{H}_{\text{ls}} = [\alpha_1 \mathbf{H}_1, \dots, \alpha_{n_{bs}} \mathbf{H}_{n_{bs}}] = \mathbf{H}_{\text{ss}} \mathbf{G} \quad (2.5)$$

is the aggregate channel matrix where the channels from the BSs to the receiver are concatenated, and large scale path losses are explicitly taken into account. The average path gain from the  $i^{\text{th}}$  BS to the receiver is  $\alpha_i$ , incorporating distance-dependent path loss and shadowing. Small-scale path gains are characterized by the matrices  $\mathbf{H}_i \in \mathbb{C}^{n_r \times n_t}$  whose entries are assumed to be i.i.d. flat Rayleigh distributed with unit variance. The aggregate small-scale path gain matrix is denoted  $\mathbf{H}_{\text{ss}} = [\mathbf{H}_1, \dots, \mathbf{H}_{n_{bs}}]$  and the large scale path gains by  $\mathbf{G} = \text{diag}(\alpha_1 \mathbf{I}_{n_t}, \dots, \alpha_{n_{bs}} \mathbf{I}_{n_t})$ . For  $\alpha_1 = \dots = \alpha_{n_{bs}}$ , the model reduces to a classical  $n_{bs}n_t \times n_s$  i.i.d. point-to-point MIMO system. We denote by  $\mathbf{V}_{\text{ls}}$  and  $\mathbf{V}_{\text{ss}} \in \mathcal{V}_{n_{bs}n_t, n_s}^{\mathbb{C}}$  the left singular vectors associated with the  $n_s$ -largest singular values of  $\mathbf{H}_{\text{ls}}^H$  and  $\mathbf{H}_{\text{ss}}^H$ , respectively.

It is assumed that the BSs know the large scale path gains of the channels contained in  $\mathbf{G}$  and the precoder is constructed in two steps. The BSs first construct a small-scale precoding matrix  $\mathbf{W}_{\text{ss}}$ . Then the large-scale precoding matrix applied is  $\mathbf{W}_{\text{ls}} = \frac{\sqrt{n_t n_{bs}}}{\|\mathbf{G}\|} \mathbf{G} \mathbf{W}_{\text{ss}}$  following the principle of adaptive precoding for correlated MIMO [54, 95]. The normalization guarantees that the total transmit power per-stream is one.

## 2.3 Codebook-Based Precoding

The channel coefficients are assumed to be perfectly known at the receiver and unknown at the transmitters. We assume that the BS has access to CSI only through an error-free, zero delay, and limited feedback channel. The precoding matrix  $\mathbf{W} \in \mathbb{C}^{n_t \times n_s}$  is designed for channel adaptation according to the information fed back by the receiver. To acquire CSI through a limited feedback channel, we consider codebook-based precoding where the receiver and transmitter share a predefined codebook  $\mathcal{C} = \{\mathbf{C}_1, \dots, \mathbf{C}_{n_{cb}}\}$ . Elements in the codebook are Stiefel matrices, i.e.  $\mathbf{C}_i^H \mathbf{C}_i = \mathbf{I} \forall i$ , which are used to quantize the eigendirections of the signal subspace at the receiver.

The receiver selects a codeword following a quantization rule that approximates the channel by using the codebook,

$$q_{\mathcal{C}} : \{\mathbf{H}\} \rightarrow \{i : 1 \leq i \leq n_{cb}\}, \quad (2.6)$$

and feeds back the index  $k = q_{\mathcal{C}}(\mathbf{H})$  to the transmitter. Then, the transmitter constructs a precoding matrix based on the CSI received, i.e.  $\mathbf{W}$  is a function of  $\mathbf{C}_i$ . Especially for point-to-point MIMO, a simplified version is to assume that the transmitter directly picks the precoding matrix from the shared codebook:  $\mathbf{W} = \mathbf{C}_k$ .

In this setting, there is typically an infinity of precoding vectors leading to the same performance, and the possible precoding vectors can be grouped into equivalence classes. It follows that the set of equivalence classes of precoding matrices is a quotient space of the Stiefel manifold. In order to have non-equivalent codewords, the codebook should be designed as a discretization of this space of equivalence classes of precoding matrices. A Stiefel precoding codebook is then generated by taking any representative in the equivalence classes.

## 2.4 Low-Complexity Constraints

Practical codebooks in industry standards have been designed according to additional constraints of interest. In our code construction, we try to address those constraints. Low implementation-complexity codebooks are typically characterized through three design constraints [51]:

1. *Equal-transmit-power per-antenna (EP)*. The antennas are used in a

power balanced manner and their average transmit power is kept at the same level. This constrains the rows in the precoding matrix to have squared norm equal to  $n_s/n_t$ .

2. *Constrained alphabet.* The alphabet of the codebook elements is restricted to a small finite alphabet in order to limit the number of multiplications and storage requirements at the receiver. Often, the alphabet is limited to the unit circle, which is also known for beamforming as equal gain transmission [52, 63]. This guarantees the EP constraint above. Restricting the alphabet to  $\{1, -1, i, -i\}$ ,  $i = \sqrt{-1}$  further reduces complexity by enabling matrix multiplications to be performed only by conjugations and additions [44, 60].
3. *Nested property.* A lower rank precoding matrix is a submatrix of a higher rank precoding matrix.

In the current 3GPP LTE-Advanced industry standard, the number of antennas at the base station may be two, four, or eight. The 2Tx codebook can be seen as an example of extraspecial group code constructions described in Chapter 5, cf. codebook B in Table I from Publication IV. For 4Tx, the LTE codebooks were designed based on Householder reflections. The resulting codebooks have similar distance properties as the codebooks of Publication IV (codebook C in Table 5.4) and thus perform equivalently in term of spectral efficiency. As discussed in [1] the implementation benefit from the Householder construction was accidental and valid only for 4Tx; it is also noted that discrete Fourier transform (DFT) codebooks fail to be a valid design for 8Tx systems. To overcome this issue, the 8Tx codebook in LTE-Advanced is constructed by concatenating the same 4Tx DFT codeword twice and using a cophasing factor [80]. The resulting codebook has a structure resembling the product codebooks considered in Publication VII.

### 3. Flag Manifolds: Code Designs and Geometry

The codebooks addressed have orthonormal columns, and can be interpreted as elements in a flag manifold with representative in a Stiefel manifold. A manifold is roughly speaking a curved space which locally resembles the Euclidean space. To investigate coding problems, we need to define a notion of distance. Depending of the application and convenience, several non-equivalent distances has been considered on these spaces [28]. We focus on *chordal distances* corresponding to natural Euclidean distances from spherical embeddings. There are two motivations for this choice. First, we are interested in computable distance functions consistent with the rectangular unitary matrix representation. Second, the considered chordal distances for Stiefel, Grassmann, and some simple flag manifolds have been shown to be related to performance of space-time codes and precoding codebooks in SU and MU-MIMO [22, 35, 47, 56]. This choice of distances enforces treatment of the manifolds as subsurfaces of hyperspheres, and implies that flag codes are a subclass of spherical codes.

#### 3.1 Flag Manifolds

The complex Stiefel manifold  $\mathcal{V}_{n_t, n_s}^{\mathbb{C}}$  is defined as the space of orthonormal rectangular matrices (with  $n_s \leq n_t$ ),

$$\mathcal{V}_{n_t, n_s}^{\mathbb{C}} = \{ \mathbf{Y} \in \mathbb{C}^{n_t \times n_s} \mid \mathbf{Y}^H \mathbf{Y} = \mathbf{I}_{n_s} \}. \quad (3.1)$$

The unitary group  $\mathcal{U}_{n_t} = \mathcal{V}_{n_t, n_t}^{\mathbb{C}}$  is a specific case of Stiefel manifold.

The flag manifold [11, 29]

$$\mathcal{F}_{n_t; s_1, \dots, s_r}^{\mathbb{C}} = \mathcal{V}_{n_t, n_s}^{\mathbb{C}} / (\mathcal{U}_{s_1} \times \dots \times \mathcal{U}_{s_r}) \quad (3.2)$$

where  $n_s = \sum_{i=1}^r s_i$ , is the set of equivalence class of  $n_t$ -by- $n_s$  Stiefel matrices where two matrices  $\mathbf{V}, \mathbf{Y}$  are equivalent if there exists a se-

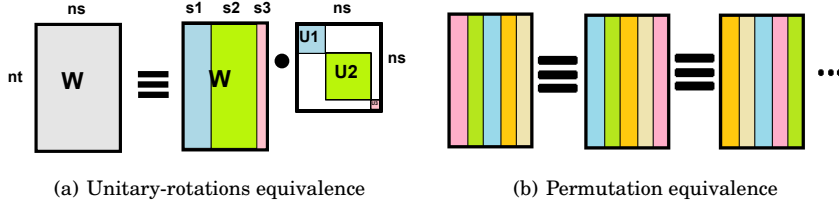


**Figure 3.1.** Illustration of the equivalence relationship considered.

quence of unitary matrices  $(\mathbf{U}_1, \dots, \mathbf{U}_r) \in (\mathcal{U}_{s_1} \times \dots \times \mathcal{U}_{s_r})$  exist such that  $\mathbf{V} = \mathbf{Y} \text{diag}(\mathbf{U}_1, \dots, \mathbf{U}_r)$ .

The case  $r = 1$  and  $s_1 = n_s$  defines the Grassmann manifold

$$\mathcal{G}_{n_t, n_s}^{\mathbb{C}} \triangleq \mathcal{F}_{n_t; n_s}^{\mathbb{C}} = \mathcal{V}_{n_t, n_s}^{\mathbb{C}} / \mathcal{U}_{n_s}, \quad (3.3)$$

which is isomorphically the set of all  $n_s$ -dimensional subspaces of  $\mathbb{C}^{n_t}$ .

According to (3.2), the Stiefel manifold  $\mathcal{V}_{n_t, n_s}^{\mathbb{C}}$  is not strictly speaking a flag manifold, but it is also a homogeneous space of the unitary group  $\mathcal{V}_{n_t, n_s}^{\mathbb{C}} \cong \mathcal{U}_{n_t} / \mathcal{U}_{n_t - n_s}$  and can be seen as an extreme case in (3.2) by setting  $r = 1$  and  $s_1 = 0$ .

Another case of interest is  $s_1 = \dots = s_r = 1$ , for which we use the notation

$$\mathcal{F}_{n_t, n_s}^{\mathbb{C}} \triangleq \mathcal{F}_{n_t; \underbrace{1, \dots, 1}_{n_s}}^{\mathbb{C}} = \mathcal{V}_{n_t, n_s}^{\mathbb{C}} / (\mathcal{U}_1)^{n_s}. \quad (3.4)$$

We finally consider an additional equivalence relationship in  $\mathcal{F}_{n_t; s_1, \dots, s_r}^{\mathbb{C}}$  when  $s_k = n_s / r$  for all  $k$ . Given  $\mathbf{V}, \mathbf{Y} \in \mathcal{V}_{n_t, n_s}^{\mathbb{C}}$ , one may group their columns in sub-matrices as  $\mathbf{V} = (\mathbf{V}_1, \mathbf{V}_2, \dots, \mathbf{V}_r)$  and  $\mathbf{Y} = (\mathbf{Y}_1, \mathbf{Y}_2, \dots, \mathbf{Y}_r)$ , such that  $\mathbf{V}_k, \mathbf{Y}_k \in \mathcal{V}_{n_t, s_k}^{\mathbb{C}}$ . Then, we consider them equivalent if they only differ by a permutation of their  $r$ -submatrices, i.e. there exists a permutation  $\sigma$  such that  $\mathbf{V} = (\mathbf{Y}_{\sigma(1)}, \mathbf{Y}_{\sigma(2)}, \dots, \mathbf{Y}_{\sigma(r)})$ . The permutation corresponds to an orientation-invariance of the elements. We denote the corresponding space by

$$\vec{\mathcal{F}}_{n_t; s_1, \dots, s_r}^{\mathbb{C}} \triangleq \mathcal{F}_{n_t; s_1, \dots, s_r}^{\mathbb{C}} / S_r \quad (3.5)$$

where  $S_r$  is the symmetric group whose elements are all the permutations of the  $r$  symbols.

Similarly for the specific case  $s_1 = \dots = s_r = 1$ , we defined

$$\vec{\mathcal{F}}_{n_t, n_s}^{\mathbb{C}} \triangleq \mathcal{F}_{n_t, n_s}^{\mathbb{C}} / S_{n_s} \quad (3.6)$$

### 3.2 Spherical Embeddings and Chordal Distances

We treat the manifolds of interest as submanifolds of hyperspheres. The spherical embeddings of the Stiefel manifold and the flag manifolds are of different natures. The Stiefel manifold has a canonical spherical embedding from the vector representation of rectangular unitary matrices. The spherical embeddings of the Grassmann manifolds with corresponding chordal distance is obtained from a projector representation [18]. In Publication VI, we show that all flag manifolds can be understood as submanifolds of the same sphere. Roughly speaking, a  $(n_t^2 - 2)$ -dimensional hypersphere can be decomposed, except for a zero-measure set, so that it consists of a “fibration” of flag manifolds  $\mathcal{F}_{n_t, n_t}^{\mathbb{C}}$  over a  $(n_t - 2)$ -dimensional hypersphere with some singular submanifolds removed. The remaining of the sphere, the singularities, correspond to other flags  $\mathcal{F}_{n_t; s_1, \dots, s_r}^{\mathbb{C}}$  which includes the Grassmann manifolds  $\mathcal{G}_{n_t, n_s}^{\mathbb{C}}$  as special cases. To generalize the notion of Grassmann distance to more general flag manifolds, we embed them into a direct product of Grassmann manifolds and take the corresponding chordal distance. This results in embedding into a larger space than the  $(n_t^2 - 2)$ -sphere. Finally, inspired by the literature in quantum information science on mutually unbiased bases (MUB) [27], we consider an alternative distance on simple permutation-invariant flag manifolds.

We have the following isometric embeddings

$$(\mathcal{M}, d_c) \hookrightarrow S^{D-1}(R) \quad (3.7)$$

where  $S^{D-1}(R) \subset \mathbb{R}^D$  is a  $(D - 1)$ -sphere of radius  $R$ , with

$\mathcal{M}$	$d_c$	$D$	$R^2$
$\mathcal{V}_{n_t, n_s}^{\mathbb{C}}$	$d_s$	$2n_t n_s$	$n_s$
$\mathcal{G}_{n_t, n_s}^{\mathbb{C}}$	$d_g$	$n_t^2 - 1$	$\frac{n_s(n_t - n_s)}{2n_t}$
$\mathcal{F}_{n_t; s_1, \dots, s_r}^{\mathbb{C}}$	$d_f$	$r(n_t^2 - 1)$	$\frac{n_s n_t - \sum_{i=1}^r s_i^2}{2n_t}$
$\vec{\mathcal{F}}_{n_t; s_1, \dots, s_r}^{\mathbb{C}}$	$d_p$	$r(n_t^2 - 1)$	$\frac{n_s n_t - \sum_{i=1}^r s_i^2}{2n_t}$
$\vec{\mathcal{F}}_{n_t, n_s}^{\mathbb{C}}$	$d_{\text{mu}}$	$\binom{n_t^2}{2} - 1$	$\frac{(n_s - 1)(n_t^2 - n_s)}{n_t^2 - 1}$

and the chordal distances, defined for  $\mathbf{Y}, \mathbf{Z} \in \mathcal{V}_{n_t, n_s}^{\mathbb{C}}$ , representatives of

their respective equivalence class, are

$$d_s(\mathbf{V}, \mathbf{Y}) = \|\mathbf{V} - \mathbf{Y}\|_F, \quad (3.8)$$

$$d_g(\mathbf{V}, \mathbf{Y}) = \frac{1}{\sqrt{2}} \|\mathbf{V}\mathbf{V}^H - \mathbf{Y}\mathbf{Y}^H\|_F, \quad (3.9)$$

$$d_f(\mathbf{V}, \mathbf{Y}) = \sqrt{\sum_{i=1}^r d_g^2(\mathbf{V}_i, \mathbf{Y}_i)}, \quad (3.10)$$

$$d_p(\mathbf{V}, \mathbf{Y}) = \min_{\mathbf{P} \in \mathcal{S}_p} d_f(\mathbf{V}, \mathbf{Y}\mathbf{P}), \quad (3.11)$$

$$d_{\text{mu}}(\mathbf{V}, \mathbf{Y}) = \sqrt{n_s - \sum_{i,j=1}^{n_s} |\mathbf{v}_i^H \mathbf{y}_j|^4}. \quad (3.12)$$

$$(3.13)$$

The decompositions of the matrices in column-blocks are given by  $\mathbf{V} = (\mathbf{V}_1, \dots, \mathbf{V}_r) = (\mathbf{v}_1, \dots, \mathbf{v}_{n_s})$  and  $\mathbf{Y} = (\mathbf{Y}_1, \dots, \mathbf{Y}_r) = (\mathbf{y}_1, \dots, \mathbf{y}_{n_s})$ . Here  $d_f$  is the metric on the flag manifold interpreted as a sequence of Grassmannians, and  $d_p$  is the permutation-invariant version. The metric  $d_{\text{mu}}$  is considered in the literature on mutually unbiased bases [27].

In Publication IV, we show also that constraining the Grassmann manifold to satisfy the EP constraint reduces the dimensionality of the spherical embedding from  $n_t^2 - 1$  to  $n_t^2 - n_t$ .

### 3.3 Codebook Designs

Several criteria have been investigated in the literature to design good MIMO precoding codebooks. With i.i.d Rayleigh fading, the right eigenvectors of the channel are uniformly distributed over the Stiefel manifold according to the Haar measure [45, 53]. As the set of eigenvectors forms a representative in a flag manifold, the set of equivalence class is also Haar distributed over this flag manifold. The main idea is to target uniform codebooks over the manifold. For this we need to define a notion of uniformity. Several mathematically non-equivalent standard criteria exist. From the point of view of precoding performance metric such as information rate, they however are almost optimal, and thus roughly equivalent [23, 56, 71, 72, 95]. For uniformity, we will consider both distortion and discrete arrangement criteria.

Consider a codebook  $\mathcal{C} = \{\mathbf{C}_1, \dots, \mathbf{C}_{n_{cb}}\} \subset \mathcal{V}_{n_t, n_s}^{\mathcal{C}}$ . Depending on the distance  $d_c$  considered, the codebook is treated as a discretization of the corresponding manifold  $\mathcal{M}$ . Consider a random source  $V$  on manifold  $(\mathcal{M}, d_c)$ ,

and define the associated quantization map

$$q_c(\mathbf{V}) = \arg \min_{1 \leq i \leq n_{cb}} d_c(\mathbf{V}, \mathbf{C}_i). \quad (3.14)$$

In quantization theory, a standard criterion is to minimize the average distortion of a codebook, i.e. the average squared quantization error,

$$D_{\mathcal{M}}(\mathcal{C}) = \mathbb{E} [d_c^2(V, \mathbf{C}_{q_c(V)})]. \quad (3.15)$$

Here, we only consider uniformly distributed source, but this criterion is adaptable for other distributions as well.

In discrete mathematics, the classical approach is to look at the properties of codebooks as point sets on the respective manifolds. The most studied criterion is maximizing the minimum distance [19, 74]

$$\delta_{\mathcal{M}}(\mathcal{C}) = \arg \min_{1 \leq i, j \leq n_{cb}} d_c(\mathbf{C}_j, \mathbf{C}_i). \quad (3.16)$$

This problem is often referred as a packing problem and is related to Tammes problem on the sphere.

A generalization of the packing problem is the Thomson problem where one has to maximize the  $p$ -mean distance [74]:

$$M_p(\mathcal{C}) = \left( \frac{2}{n_{cb}(n_{cb} - 1)} \sum_{1 \leq j < k \leq n_{cb}} d_c(\mathbf{C}_j, \mathbf{C}_k)^p \right)^{1/p}. \quad (3.17)$$

Typical values of interest are  $p = -1$  and  $-2$ .

### 3.4 Lloyd's Algorithm and Centroids

Lloyd's algorithm aims to construct a codebook with minimum average distortion. It comprises two key steps:

*Nearest Neighbor rule:* Partitioning of the manifold according to the codebook in  $n_{cb}$  Voronoi cells  $\{\mathcal{R}_1, \dots, \mathcal{R}_{n_{cb}}\}$  defined by

$$\mathcal{R}_k = \{\mathbf{V} \in \mathcal{M} \mid k = q_c(\mathbf{V})\}. \quad (3.18)$$

*Centroid Computation:* Finding the centroids of each Voronoi cell  $\mathcal{R}_k$  given by

$$\mathbf{Z}_k = \arg \min_{\mathbf{V} \in \mathcal{M}} \mathbb{E} [d_c^2(V, \mathbf{V}) \mid V \in \mathcal{R}_k]. \quad (3.19)$$

The algorithm consists of iterating these two steps where the former codebook is replaced by the set of computed centroids.

Generally, the centroid of a Voronoi cell is approximated through exhaustive search. Meanwhile, due to the treatment of the manifolds as



subspaces of Euclidean hyperspheres with canonical extrinsic distances, the centroids may also be computed in closed-form. As the manifolds are closed continuous surfaces in an Euclidean space, a centroid of a Voronoi region is obtained from the orthogonal projection onto the manifold of its center of mass in the ambient space [26]. Accordingly, we provide an exact centroid computation for the Stiefel manifold in Publication VII, where an orthogonal projection of any complex matrix to the Stiefel manifold is given by the polar decomposition following [31,41]. A closed-form solution was already known for centroids in the Grassmann manifold [58]. While the closed-form Grassmannian centroid computation is usually proven differently in the literature, it could also be derived using the argument in [26]. The centroid corresponds to the closest projection matrix of a given rank to the center of mass in the ambient space of Hermitian matrices. For deriving centroids in other flag manifolds, the main difficulty lies in expressing the orthogonal projection. In Publication VIII, the centroid for simple permutation-invariant flag manifolds was approximated through projection in the embedding space of direct product of Grassmannians, a similar approach can be found in [77]. We conjecture that this is the true centroid.

### 3.5 Density and Packing Bounds

In the last decade, basic coding-theoretic results estimating the relationship between the cardinality and the minimum distance of codes in Grassmann and Stiefel manifolds have been widely studied [7–10, 21, 22, 36, 40, 49, 50]. The Hamming bound, a standard coding bound, is related to the notion of density of codes. In Publications I and II, we discuss the density of codes in Grassmann and Stiefel manifolds equipped with a chordal distance. There are two main difficulties in evaluating the density of codes in these spaces: 1) evaluating the (normalized) volume of a ball 2) estimating the kissing radius of codes.

*1) Volumes:* The authors of [22] were able to derive closed-form expression on the volume of a small ball in Grassmannians under the chordal distance. A more general approach was used in [49, 50] where a power series expansion of the (unnormalized) volume of small ball valid for any Riemann manifold [33] was leveraged. This provides a powerful tool—in order to obtain a normalized volume expansion, it suffices to divide by the overall volume of the manifold. The volume of the manifold depends of

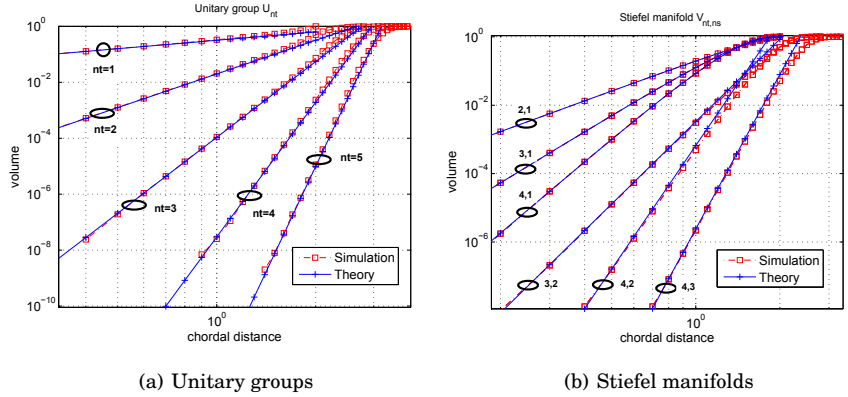


**Figure 3.2.** Volume approximation of balls in Stiefel manifolds and unitary groups compared to simulation.

the Riemannian metric defining the notion of distance. There is an equivalent intrinsic Riemannian metric corresponding to the extrinsic chordal distance. In fact, from the Nash embedding theorem, every Riemannian metric can be seen as being induced by an appropriate Euclidean embedding [65]. For the case of the Stiefel manifold, two non-equivalent Riemannian metrics are often considered [28], one realized from the space of rectangular unitary matrices and the other from the interpretation of the manifold as a quotient space of the unitary group embedded in the space of square unitary matrices. It appears that in the majority of the literature, the volumes of the manifolds do not correspond to any of these two metrics. Indeed, the volume element is unique up to a non-vanishing scaling factor which is often dismissed, as it can be absorbed in the overall normalization. Here, the volume expansion imposes the scaling of the metric and volume element. For accurate normalization of the expansion of [33], the volume of the manifold should be calculated with the same metric. A discussion and clarification of different conventional normalizations of the volume of the unitary group is provided in [98]. In [49] the volume of the complex Stiefel manifold is computed for the geodesic distance induced by the quotient geometry. In Publication II, we address the problem when considering the typical chordal distance induced by the rectangular matrix embedding, which leads to an expression of the volume differing from the ones previously derived in [49] or [40]. The exact volume of the Grassmann manifold with chordal distance is also computed. A corresponding volume computation and mindmap is presented in Fig. 3.3. The exactness of the volume is illustrated in the estimation of volume of small ball for the Stiefel manifolds and unitary groups in Fig. 3.2.

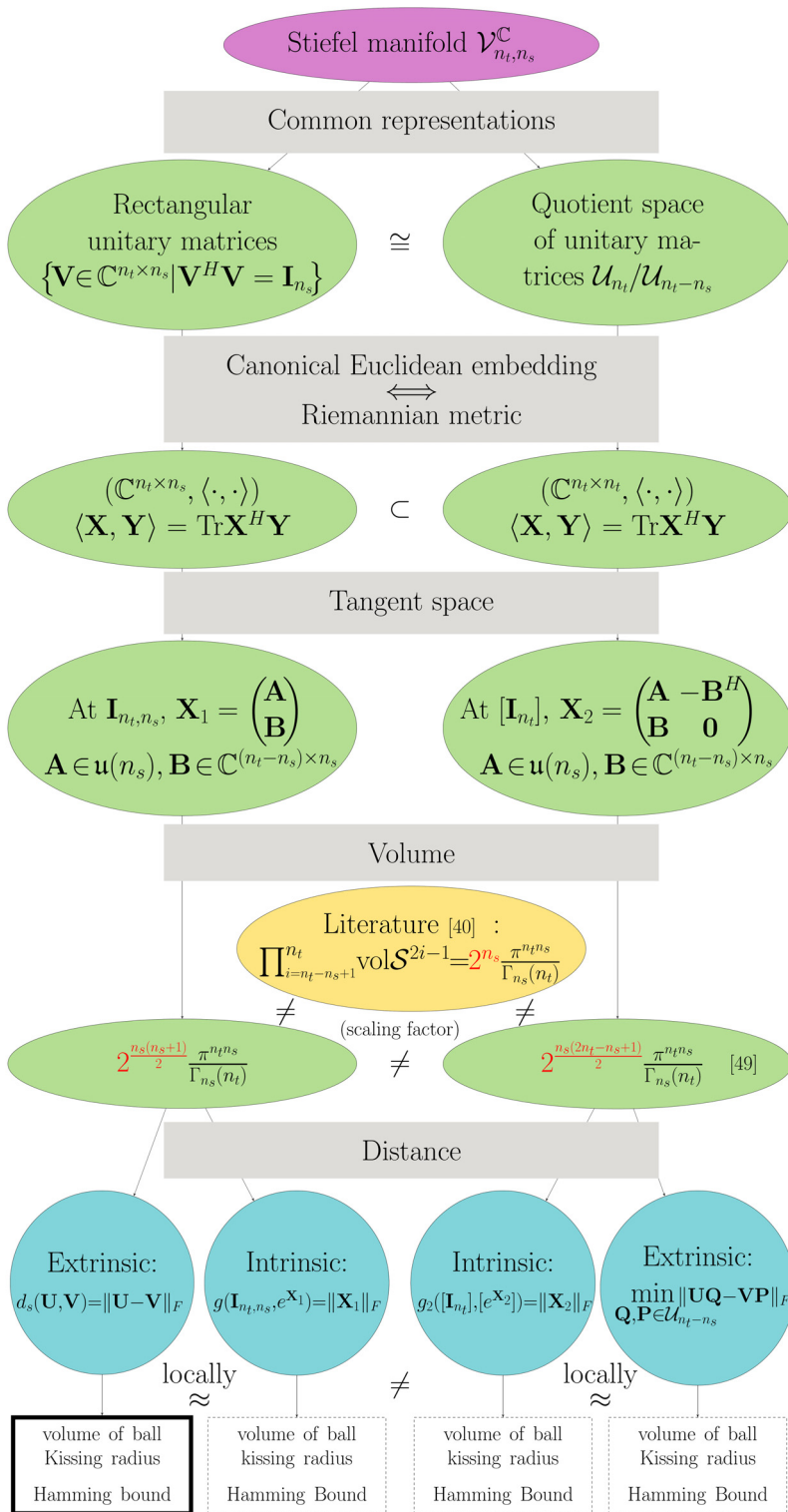


**Figure 3.3.** Choice of distance and its impact on volume computation and coding bounds for Stiefel manifolds.

2) *Kissing Radius*: As we are considering extrinsic distances, there is room for improvement of the standard Hamming bound [9, 36] through the notion of density. We address this problem for the Grassmann manifold in Publication I and for any spherically-embedded manifold in Publication II. The density of a code is defined as the fraction of the manifold covered by ‘kissing’ balls of equal radius centered around the codewords. The kissing radius problem addresses the following question: if two points are at chordal distance  $\delta$ , how far is the midpoint from the extremities. For a geodesic distance, the answer is simply  $\delta/2$ ; with an extrinsic distance, this is greater than  $\delta/2$ . While there is a unique and exact answer to this question on a sphere, this is not the case for flag and Stiefel manifolds with chordal distances, because in general these spaces are not two-point homogeneous. For these, the kissing radius cannot be determined solely from the minimum distance. We provide upper and lower bounds on the kissing radius as a function of minimum distance for the Grassmann and Stiefel manifold in Publications I and II.

3) *Packing Bounds*: Bounds on the kissing radius leads to a refinement of the standard Hamming bound for flag and Stiefel codes. Based on this, Publication I provides new bounds on the minimum Grassmann distance. In Publication II, we provide a similar bound for any spherically-embedded manifold generalizing previously known bounds on codes in the unitary group [36] to the Stiefel manifold:

*Given a code of cardinality  $n_{cb}$  and minimum chordal distance  $\delta_{\mathcal{M}}$  in a manifold  $\mathcal{M}$  isometrically embedded in  $S^{D-1}(R)$ , we have*

$$\delta_{\mathcal{M}}^2 \leq 4r_n^2 - \frac{r_n^4}{R^2}, \quad (3.20)$$

where  $r_n$  is solution of  $\mu(B(r_n)) = \frac{1}{n_{cb}}$  and  $\mu(B(r_n))$  is the normalized volume of a ball of radius  $r_n$ .

Applying this result to the unitary group leads to the bound [36, Theorem 2.4]. A tighter bound is provided for a small range of large distances by [36, Corollary 2.9]. In Publication I, for Grassmann manifolds, we were able to improve the bound by

$$\delta_g^2 \leq 4r_n^2 - \frac{r_n^4}{n_s}, \quad (3.21)$$

which is a generalization of the bound in [96] valid only for line packing ( $n_s = 1$ ).

The Hamming bound is rather loose especially for small codes. For low cardinality, Rankin bounds [70] related to the spherical embeddings

are known to be tight when applied to Grassmann codes [18]. In a  $D$ -dimensional sphere, the optimum packings for up to  $D + 1$  points corresponds to simplices. From  $D + 2$  to  $2D$  points, the optimal configurations are subsets of an orthoplex. They are thus referred as simplex and orthoplex bounds, respectively [18].

As discussed in Publication IV, the smaller embedding provided for EP codebooks leads to a modification of the range of the Rankin bounds. The corresponding EP orthoplex bound is used for proving the optimality of some of the packings presented in Publication IV.

## 4. Grassmannian Pakings for 2-Tx MIMO

The lowest dimensional flag manifolds ( $n_t = 2$ ) are very specific cases. We have  $\mathcal{F}_{2,2}^{\mathbb{C}} \cong \mathcal{F}_{2,1}^{\mathbb{C}} \cong \mathcal{G}_{2,1}^{\mathbb{C}}$ , which further reduces to the real unit sphere  $\mathcal{F}_{2,2}^{\mathbb{C}} \cong S^2$ . It follows that designing codebooks in  $\mathcal{F}_{2,2}^{\mathbb{C}} \cong \mathcal{G}_{2,1}^{\mathbb{C}}$  is equivalent to designing spherical codes. In this chapter, we discuss explicit representation of spherical codes in 2-by-1 vector form for coding in  $\mathcal{G}_{2,1}^{\mathbb{C}}$ ; equivalent 2-by-2 matrix codes for  $\mathcal{F}_{2,2}^{\mathbb{C}}$  can be obtained by pairing an orthogonal complement of each codeword. In addition, a  $2 \times 2$  unitary matrix generating a point in  $\mathcal{F}_{2,2}^{\mathbb{C}}$  can be seen as two ordered antipodal points, or equivalently an oriented line. It follows that  $\mathcal{F}_{2,2}^{\mathbb{C}}$  is the set of spherical antipodal points, or equivalently the set of lines in 3D, also known as the real Grassmannian  $\mathcal{G}_{3,1}^{\mathbb{R}} \cong \mathcal{F}_{2,2}^{\mathbb{C}}$  [18]. Codebooks in  $\mathcal{F}_{2,2}^{\mathbb{C}}$  can thus be constructed by leveraging results from known antipodal spherical codes [57].

### 4.1 Grassmannian Codebooks from Spherical Arrangements

The Grassmann manifold  $\mathcal{G}_{2,1}^{\mathbb{C}}$  is by definition the *complex projective line*  $\mathbb{C}P^1$ . From the Hopf fibration of the unit 3-sphere as a circle bundle over  $\mathbb{C}P^1$  [12, Ex.17.23], we have

$$\mathcal{G}_{2,1}^{\mathbb{C}} = \mathbb{C}P^1 \cong \frac{S^3}{S^1} = S^2. \quad (4.1)$$

For the explicit form of the isomorphism we parameterize the unit vector  $\mathbf{w}$ , a generator of the equivalence class  $[\mathbf{w}] \in \mathcal{G}_{2,1}^{\mathbb{C}}$ , as

$$\mathbf{w}(\theta, \phi) = \begin{pmatrix} \cos \theta \\ e^{i\phi} \sin \theta \end{pmatrix}. \quad (4.2)$$

By setting the range of  $\theta$  and  $\phi$  to  $[0; \frac{\pi}{2}]$  and  $[0; 2\pi]$ , respectively, we fully describe the Grassmannian. Interpreting  $(\theta, \phi)$  directly as spherical coordinates, these would describe a hemisphere. A simple morphism from a

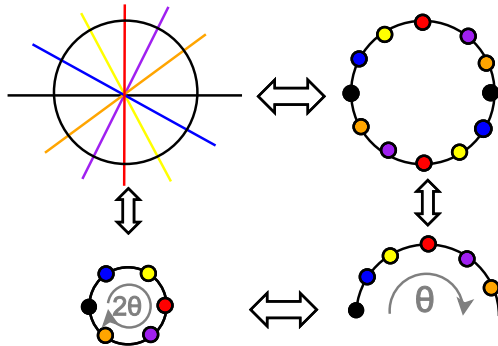


**Figure 4.1.** The real Grassmannian  $\mathcal{G}_{2,1}^{\mathbb{R}}$  is the set of lines in  $\mathbb{R}^2$ , or equivalently the set of antipodal points on the unit circle. Taking only representatives on the upper hemisphere, an isometry to a circle is obtained by doubling the parametric angle  $\theta$  and reducing the radius to one half.

hemisphere to the whole sphere can be obtained by doubling the angle  $\theta$ . The irrelevance of  $\phi$  for  $\theta = 0$  and  $\frac{\pi}{2}$  in (4.2) leads to the isomorphism.

Moreover, with the chordal distance considered,  $\mathcal{G}_{2,1}^{\mathbb{C}}$  is isometric to the real sphere (of radius one half). Isometry implies that discretization problems on  $(\mathcal{G}_{2,1}^{\mathbb{C}}, d_g)$  can be addressed on the the real sphere  $S^2$ . Any spherical code can be transformed to a Grassmannian codebook by applying the corresponding simple change of variables. Cartesian coordinates are first converted to spherical coordinates  $(\vartheta, \phi)$  and the latitude is divided by two ( $\theta = \frac{\vartheta}{2}, \phi$ ). A generator of the corresponding Grassmannian line is then obtained by using  $(\theta, \phi)$  in (4.2). As a result, the chordal distance between two Grassmannian lines is half the distance between the respective spherical codewords. We illustrate this isometry for  $\phi = 0$  which corresponds to the real Grassmannian  $\mathcal{G}_{2,1}^{\mathbb{R}} \cong S^1$  isomorphic to a circle in Fig. 4.1.

The problem of distributing a certain number of points uniformly over the surface of a sphere has been thoroughly studied [74]. Different criteria on the mutual distances among the codewords have been extremized in the literature, with motivation often arising from chemistry, biology and physics [19, 74, 92]. For convenience, solutions are often described as the vertices of a convex polyhedron.

The *Tammes problem* is the problem of placing  $n_{cb}$  points on a sphere so as to maximize the minimum distance, also referred to as *spherical packing*, is a specific case of spherical arrangements [74]. It follows that Grassmannian line packing in  $\mathcal{G}_{2,1}^{\mathbb{C}}$  is equivalent to the Tammes problem. In Publication III, we have thus construct codebooks and leverage existing results from the spherical code literature by using the isometry.

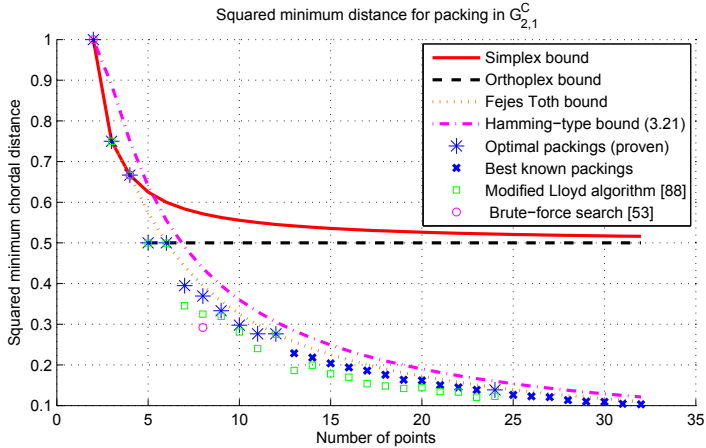


**Figure 4.2.** Best known squared minimal chordal distance for packings in  $\mathcal{G}_{2,1}^C$ .

The Rankin bounds [70] and the Fejes Tóth bound [30] applies to the minimum distance of packings in  $\mathcal{G}_{2,1}^C$ . The Fejes Tóth bound is specific for the 2-sphere. It is tighter than the Hamming-type bound (3.21) which in this case reduces to the bound in [96]. These bounds lead to proof of optimality of some packings. Optimum packings of  $n_{cb}$  points on a sphere have been found for  $n_{cb} \leq 12$  and  $n_{cb} = 24$  [17, 30], with optimality proven geometrically. For  $n_{cb}$  up to 130, the best known sphere packings are available at Sloane's webpage [84]. Fig. 4.2 shows the achieved minimum distances of the corresponding Grassmannian packings along with bounds, compared to numerical results from [94, 96] where a modified Lloyd search algorithm was used and to results from [56] using brute-force computer search.

The problem of maximizing the generalized  $p$ -mean of the mutual distances among the codewords can be called the *generalized Thomson problem*. It is the counterpart of a spherical arrangement problem which, due to its relevance to physics, is often formulated as the minimization problem of the Riesz  $s$ -energy for  $s > 0$ . It is remarked in [74] that on  $S^2$  this problem is only interesting for  $p < 2$ .

Some values of  $p$  have attracted special interest. The case  $p = -1$  (sometimes also  $p = -2$ ) is known as the (standard) *Thomson problem*. Solutions referred to as *Fekete points* have been found for  $n_{cb} = 2-4, 6, 12$  [25]. Another distinguished problem is the problem of maximizing the product of the distances, known as *Whyte's problem*. This occurs when  $p \rightarrow 0$  and can be restated equivalently as minimizing the logarithmic energy. So-



lutions referred to as *logarithmic points* have been found for  $n_{cb} = 2-6, 12$  [25]. The limiting case  $p \rightarrow -\infty$  is the Tammes Problem discussed above.

These problems are not in general solved by identical arrangements. However due to the high symmetry of the optimum solutions of Tammes problem for 2-4, 6 and 12 points, these cases are conjectured to provide general solutions [25, 74, 92]. The principal approach to solve these problems on  $S^2$  has been to use extensive numeric computations, especially in high cardinality. Results may be found at [38, 84] for  $p = -1$  and  $-\infty$  respectively, and at [13] for  $p$  from 0 to  $-12$ .

In [37], a library of  $n_{cb}$ -point arrangements on a sphere that maximize the volume of the convex hull is also available. These may also be used as a basis for constructing precoding codebooks.

## 4.2 Low Implementation-Complexity Codes

Most solutions of spherical arrangement problems are vertices of polyhedra with a high degree of symmetry which makes the derivation of closed-form Grassmannian codebooks possible. One benefit of having geometric insight on the codebooks, and the corresponding analytical handle on their design, is that suitable rotations can be found by geometric inspection. Such rotations can be used to simplify the representation of the codebook. This is beneficial from several perspectives. First, the codebook can be rotated so that it can be realized with a minimum number of different complex numbers without impairing performance. Typically, selection of the precoding codeword is done at the receiver by exhaustive search over all codewords in the codebook. Codebooks with arbitrary complex entries result in many complex multiplications at the receiver. Reduced computing complexity, as well as reduced storage, is possible by constraining the entries to a finite alphabet. Also, analytic control on the codebooks may be used to select how the codebooks distribute power across the antennas. Finally, analytic control of the codebooks, together with geometric intuition, allows investigating non-optimum codebooks, with possibly different symmetry properties than the optimum ones, in order to balance performance, storage and computing complexity.

In Publication III, we derived simple closed form codebooks from spherical arrangements with up to 5 bits. Of particular interest are the codebooks with  $n_{cb} = 2, 4, 8$  and 16 codewords, i.e. the 1-, 2-, 3- and 4-bit

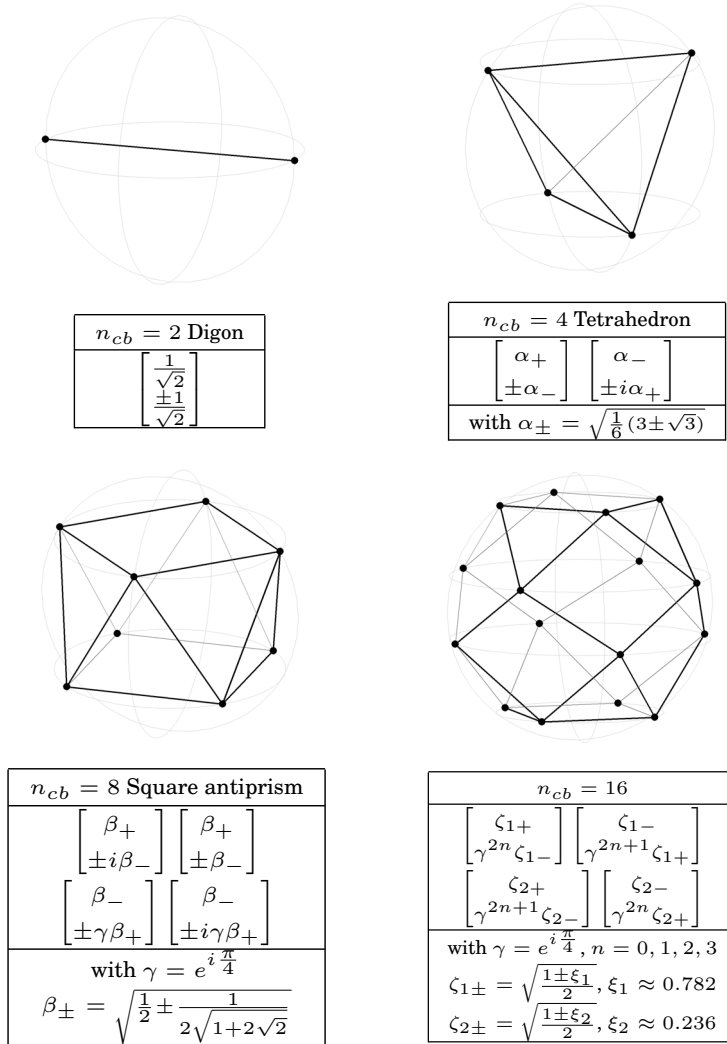


**Figure 4.3.** Digon, tetrahedron, square antiprism and 4-bit spherical arrangement.

codebooks. These polyhedra are depicted in Fig. 4.3.

The codebooks in Fig. 4.3 have been rotated in order to decrease search and storage complexity. To illustrate the implementation benefit of the closed-form representation, Table 4.1 gives a comparison in terms of the required number of multiplications and storage bits between random, or numerically found codebooks, and the 1-, 2-, 3- and 4-bit codebooks of Fig. 4.3. The required number of complex entries generating the codebooks has been decreased by rotating them so that several points are on the same latitude. Furthermore, if longitudinal separation between points on the same latitude are  $\pi$ ,  $\pi/2$ ,  $\pi/4$  or a multiple of those, some

**Table 4.1.** Implementation complexity.

$n_{cb}$	Number of multiplications		Storage bits	
	Proposed CBs	Random CBs	Proposed CBs	Random CBs
2	0	12	2	$6K_b$
4	4	28	$K_b + 21$	$14K_b$
8	6	60	$2K_b + 28$	$30K_b$
16	6	124	$4K_b + 42$	$62K_b$

complex multiplications can be reduced either to a sign change, a swap between the real and imaginary parts, additions, or a combination of such. Additionally, complexity of a codebook can be slightly decreased by scaling it so that the first entry of the first codeword is equal to one. Taking the Tetrahedron codebook as an example, this gives  $\{(1, \pm c), (c, \pm i)\}$  with  $c = \alpha_-/\alpha_+$ , thus only one real value,  $c$ , needs to be stored, and only four real multiplications are needed in total. On the other hand, if the entries of the codebook are arbitrary complex numbers, each inner product between two vectors requires height real multiplications, and storage of four real values. In summary, with a random codebook of  $n_{cb}$  codewords, the required number of multiplications is  $4(2n_{cb} - 1)$ , and the number of bits required for storage is  $2(2n_{cb} - 1)K_b$ , where  $K_b$  is the number of bits needed to represent a real number.

### 4.3 Quantization Error Analysis

Since we have designed codebooks analytically, we may be able to compute the pdf and the average of the squared quantization error in closed form. For beamforming, the squared quantization error corresponds to a SNR loss. This can be computed from the interpretation as spherical code. The pdf of the quantization error is given by

$$f_{d_g^2}(z) = \frac{1}{2\pi} \sum_{k=1}^{n_{cb}} \int_{\mathcal{C}_k(z) \cap \mathcal{R}_k} d\phi_k. \quad (4.3)$$

where  $\mathcal{R}_k$  is the Voronoi cell of the  $k^{th}$  codeword, and

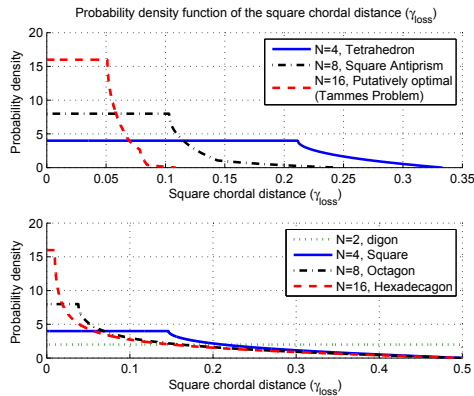
$$\mathcal{C}_k(z) = \{\mathbf{v} \in S^2(\frac{1}{2}) : |\mathbf{v} - \mathbf{c}_k|^2 = z\}.$$

is the border of a spherical cap of squared radius  $z$  centered at codeword  $\mathbf{c}_i$ .

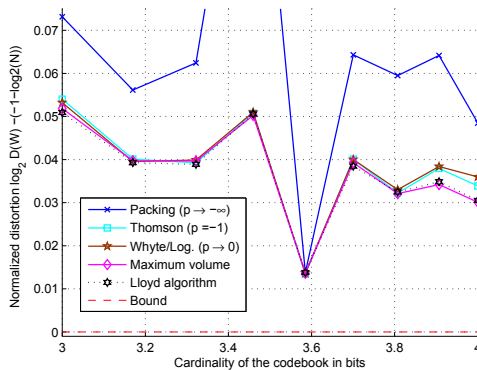
The integral in the last equality can be calculated by taking into account the fact that the discontinuities of  $\mathcal{C}_i(z) \cap \mathcal{R}_i$  belong to the borders of  $\mathcal{R}_i$ . The borders of  $\mathcal{R}_i$  are geodesics which may be expressed by a goniometric equation [67].

We have performed explicit calculations of  $f_{d_g^2}$  for the codebooks of size 1, 2, 3 and 4 bits of the best known Grassmannian packings provided of Fig. 4.3. These pdfs are drawn in Fig. 4.4(a). For EP codebooks, analytical expressions for the pdf of the SNR loss, calculated relative to perfect equal gain beamforming, are given in [63].

Figure 4.4(a) gives a comparison of the average quantization error obtained from different spherical arrangement. The performance of the maximum volume configurations coincides with the best results found by Lloyd's algorithm. The packing solutions perform slightly worse in general. In term of precoding performance, this corresponds to a loss in average SNR of the order of  $10^{-3}$  dB – i.e. the difference is insignificant.



(a) Pdfs



(b) Relative mean squared quantization error

**Figure 4.4.** Pdfs and mean squared quantization error from constructed codebooks.



## 5. Flag and Stiefel Orbit Codes

Most good codes of Chapter 4 have a natural interpretation as orbits of a symmetry group [19, 30]. Orbit constructions for unitary codes has not been widely addressed [66]. Seminal results exist for spherical codes [81, 82]. In [78], unitary codes were constructed from the representation of fixed-point-free groups, corresponding to an orbit of the identity element. Along this line, some Stiefel codes were constructed in [34]. For Grassmann codes, few works have been addressing group orbit constructions [15, 18, 20].

In this chapter, we use group orbits to construct codes in flag and Stiefel manifolds. Flag orbits are constructed by acting with a unitary representation of a finite group. In the construction, the center of the finite group has no effect, and thus it is sufficient to consider its inner automorphism group. Often, orbit construction generates structured codes with finite input alphabet, which is beneficial for hardware implementation of MIMO precoding. In this regards, a construction based on the structure of extraspecial groups, leading to orbits of Clifford groups, is of specific interest. Other explicit constructions from projective unitary representations of finite groups are also described. We also give examples of codes on the Stiefel manifold constructed as orbits of the linear representation of projective groups, which are thus expansions of the flag codes considered.

### 5.1 Orbits of Projective Group Representations

Consider a finite unitary group  $G \subset \mathcal{U}_{n_t}$  acting on  $\mathcal{V}_{n_t, n_s}^{\mathbb{C}}$  and thus on quotient spaces of it. Given a group  $G$  and a initial point  $[\mathbf{Y}]$ ,  $\mathbf{Y} \in \mathcal{V}_{n_t, n_s}^{\mathbb{C}}$ , in the manifold of interest, the orbit of  $[\mathbf{Y}]$  under the action of  $G$  is the subset

$$G[\mathbf{Y}] = \{[g\mathbf{Y}] \mid g \in G\}. \quad (5.1)$$

We shall see that groups with projective representations are of specific interest for flag orbit construction. The center of the unitary group  $\mathcal{U}_{n_t}$  is  $Z(\mathcal{U}_{n_t}) = \{e^{i\theta}\mathbf{I}_{n_t} \mid \theta \in \mathbb{R}\} \cong \mathcal{U}_1$ . The *projective unitary group* is the quotient of the unitary group by its center  $\mathcal{PU}_{n_t} = \mathcal{U}_{n_t}/Z(\mathcal{U}_{n_t})$ . An element in  $\mathcal{PU}_{n_t}$  is an equivalence class of unitary matrices under multiplication by a constant phase. If a group can be homomorphically mapped to  $\mathcal{PU}_{n_t}$ , it is said to have a projective unitary representation. Such can be naturally understood in terms of a linear representation of  $\mathcal{U}_n$  acting on projection operators by conjugation.

Given a group  $G$  having a faithful irreducible representation in  $\mathcal{U}_{n_t}$ , its inner automorphism group  $\text{Inn}(G)$  has a representation in  $\mathcal{PU}_{n_t}$ . In Publications V and VI, we show that *flag orbits of the action of  $G$  are orbits of the action of  $\text{Inn}(G)$* : for any  $[Y] \in \mathcal{F}_{n_t; s_1, \dots, s_r}^{\mathbb{C}}$ , we have  $G[Y] = \text{Inn}(G)[Y]$ . It follows that to construct flag orbit codes, we are primarily interested by groups having a representation in  $\mathcal{PU}_{n_t}$ .

The cardinality of the orbit code depends on the size of the stabilizer subgroup of the initial point in  $G$ . Initial points with trivial stabilizer leads to orbit codes of the same cardinality as the group. For manifolds without permutation equivalence, this holds for almost every point in the manifold. When the group has permutation elements, no point in  $\vec{\mathcal{F}}_{n_t, s_1, \dots, s_r}^{\mathbb{C}}$  has trivial stabilizer. Initial points leading to orbit codes of size less than the group size have by definition a stabilizer which is a non-trivial subgroup of  $G$ . These are singularities in the manifold and there is only a finite number of such codes. Such initial points in  $\mathcal{F}_{n_t; s_1, \dots, s_r}^{\mathbb{C}}$  are concatenations of  $r$  invariant subspaces of dimension  $\{s_1, \dots, s_r\}$  of some non-trivial subgroup of  $G$ . In this case, appropriate initial points can be found from eigenspaces of the matrix representation of the group.

In Publication V, we derive some basic properties of Grassmann orbit codes and describe explicit constructions of group orbits leading to some optimum packings in 2 and 4 dimensions. Recall that the Grassmann manifold  $\mathcal{G}_{n_t, n_s}^{\mathbb{C}}$  equipped with the chordal distance is isometrically embedded onto a sphere in an Euclidean space of dimension  $n_t^2 - 1$ . Any finite group represented in  $\mathcal{PU}_{n_t}$  acts on the basis of this Euclidean space and is a subgroup of the orthogonal group  $\mathcal{SO}_{n_t^2 - 1}$ . Except for  $n_t = 2$ , where  $\mathcal{SO}_3 \cong \mathcal{PU}_2$ ,  $\mathcal{SO}_{n_t^2 - 1}$  is larger than  $\mathcal{PU}_{n_t}$  and thus we cannot realize all the rotations of the Euclidean space with this projective representation. In 2D, we give explicit constructions of group orbits recovering the optimum packings of Publication III. For higher dimension, we look for groups

**Table 5.1.** Orbit codes in  $\mathcal{G}_{2,1}^{\mathbb{C}}$  of cardinality  $n_{cb}$  and minimum squared distance  $\delta_g^2$ .

Group	Order	$n_{cb}$	$\delta_g^2$	Polyhedron
$V_4 \cong \text{Inn}(D_8)$	4	2	1	Digon (optimum)
		4	$\frac{2}{3}$	Tetrahedron (optimum)
$S_3$	6	2	1	Digon (optimum)
		3	$\frac{3}{4}$	Triangle (optimum)
		6	$\frac{1}{2}$	Octahedron (optimum)
$D_8 \cong \text{Inn}(D_{16})$	8	4	$\frac{1}{2}$	Square
		8	$\frac{4-\sqrt{2}}{7}$	Square antiprism (optimum)
$T \cong A_4 \cong \text{Inn}(2T)$	12	4	$\frac{2}{3}$	Tetrahedron (optimum)
		12	$\frac{\sqrt{5}-1}{2\sqrt{6}}$	Icosahedron (optimum)
$O \cong S_4 \cong \text{Inn}(2O)$	24	6	$\frac{1}{2}$	Octahedron (optimum)
		8	$\frac{1}{3}$	Cube
		24	$\approx 0.1385$	Snub cube (optimum)

**Table 5.2.** Codes from Clifford group in  $\mathcal{G}_{4,2}^{\mathbb{C}}$  of cardinality  $n_{cb}$  and minimum squared distance  $\delta_g^2$ .

$n_{cb}$	$\delta_g^2$	% HB	Comments
30	1	66	Orthoplex (optimum). Similar than in [4].
120	0.75	64	Subset of 320-orbit
320	0.44	46	
360	0.5	53	
390	0.5	54	Union of 30- and 360- orbits. Similar than in [4].
480	0.32	36	Subset of 1440-orbit
710	0.44	54	Union of 30-, 320-, and 360- orbits
1440	0.2	29	
2150	0.2	31	Union of 30-, 320-, 360-, and 1440- orbits

that have a relatively simple action on the basis. The Clifford group employed in quantum information theory permutes and rotates the basis of the considered space. It is thus natural to consider the Clifford group for codebook generation. Furthermore, in Publication V we describe several constructions arising from the Clifford group in 4D, recovering some codes from [4]. The results are summarized in Table 5.1 and 5.2. In Table 5.2, the squared minimum distance of the code is evaluated in percentage of the Hamming-type bound (3.21). The low-cardinality finite groups used are the Klein Group  $V_4$ , the symmetric group  $S_3$ , the dihedral group  $D_8$ , the tetrahedral group  $T$  and the octahedral group  $O$ . Some codes meet the Rankin bounds. Other justifications of optimality for codes in  $\mathcal{G}_{2,1}^{\mathbb{C}}$  can be found in Publication III.



**Table 5.3.** Some  $(n_{cb}, \delta^2)$ -flag orbit codes.

$\tilde{\mathcal{F}}_{2,2}^{\mathbb{C}}$			$\tilde{\mathcal{F}}_{4,4}^{\mathbb{C}}$		
$n_{cb}$	$\delta_p^2$	$\delta_{\text{mu}}^2$	$n_{cb}$	$\delta_p^2$	$\delta_{\text{mu}}^2$
			15	2	2
3	1	1	90	1	1
4	0.66	0.88	180	0.59	1
6	0.55	0.8	360	1.25	1.75
15	0.19	0.35	960	0.5	0.75
			1440	0.22	0.40

In Publication VI, we give examples of orbit codes in other flag manifolds. Their cardinality and squared minimum flag distances are given in Table 5.3, where  $\delta_p$  and  $\delta_{\text{mu}}$  are the minimum distance according to (3.11) and (3.12), respectively.

Designing codes in the lowest dimensional flag manifolds  $\mathcal{F}_{2,2}^{\mathbb{C}} \cong \mathcal{F}_{2,1}^{\mathbb{C}} \cong \mathcal{G}_{2,1}^{\mathbb{C}} \cong S^2$  and in  $\tilde{\mathcal{F}}_{2,2}^{\mathbb{C}} \cong \mathcal{G}_{3,1}^{\mathbb{R}}$  is again equivalent to designing spherical codes and in  $\tilde{\mathcal{F}}_{2,2}^{\mathbb{C}} \cong \mathcal{G}_{3,1}^{\mathbb{R}}$  antipodal spherical codes, respectively. Some optimal orbit codes in  $\tilde{\mathcal{F}}_{2,2}^{\mathbb{C}}$  can be obtained by pairing antipodals of orbit codes in  $\mathcal{G}_{2,1}^{\mathbb{C}}$ . Examples of optimal orbit codes are simplices of cardinality 3 and 4, orbits of the octahedral group  $O$ , forming an octahedron and a cube on the sphere. The maximum simplicial configuration, i.e. of cardinality 6, forms an icosahedron, an orbit of the tetrahedral group. As expected, the mutual unbiasedness distances  $\delta_{\text{mu}}$  for these codes match the result of [18], meeting the Rankin bound. A suboptimal packing of size 15 is also given as orbit of the icosahedral group  $A_5$ , inner automorphism group of the binary icosahedral group  $2I$ . The obtained squared mutual unbiasedness distance is 0.35, for comparison the putatively optimum code has  $\delta_{\text{mu}}^2 \approx 0.38$ .

We also provide construction in  $\tilde{\mathcal{F}}_{4,4}^{\mathbb{C}}$  from orbits of the Clifford Group. In this space, code elements are  $4 \times 4$  unitary matrices modulo column permutations and columnwise rotations. From the eigenvectors of the group elements, we found some initial points with non-trivial stabilizers of different orders. The resulting codes with cardinality and minimum distance are presented in Table 5.3. From the table, one can notice that the two considered distance functions behave quite similarly except for the code of size 180. The generator of the 15-points codes is the identity matrix, i.e. the code corresponds to taking the finite group directly as a code itself. This code is a collection of 3 maximal set of mutually unbiased

bases [27]. To a  $(n_{cb}, \delta_p^2)$ -codes in  $\bar{\mathcal{F}}_{4,4}^{\mathbb{C}}$ , shown in Table 5.3, there exists a corresponding  $(24n_{cb}, \delta_p^2)$ -code in  $\mathcal{F}_{4,4}^{\mathbb{C}}$ .

## 5.2 Extraspecial Group Code Constructions

In Publication IV, a construction of Grassmannian packings related to representation theory is applied to build implementation-friendly codes when the number of transmit antennas is a power of a prime number. The codes are multimodal and can be generated from a finite alphabet consisting of roots of unity. Moreover, their cardinality can be decreased in order to meet an equal power per antenna constraint.

The construction is based on a group-theoretic framework for packings in the real Grassmannian, provided in [15] for dimensions that are powers of 2. This framework is based on the properties of *extraspecial 2-groups* [14]. In Publication IV, this construction is generalized to the complex Grassmannian and for any power of a prime  $p$ , based on the extensions to extraspecial  $p$ -groups in [14]. For dimensions that are powers of 2, the construction is a specific case of the constructions presented in [3–6] for non-coherent MIMO and MIMO broadcasting. Whereas in [3–5] the construction is generalized to construct larger codes, in Publication IV, we look for smaller codes with good implementation properties. The generalization to any prime was also done independently in [73].

The main idea is to look for abelian subgroups that are different representations of the same group. The subgroups are actually images of an orbit under the action of the Clifford group. As representations of an abelian group are reducible to one-dimensional representations, one can connect every subgroup with a corresponding decomposition of the representation space into orthogonal lines, representable by a unitary matrix. The codes consist of collections of these orthogonal bases and subspaces spanned by them. As a by-product, the obtained codes are orbits of the Clifford group, and can also be constructed as such. The extraspecial group machinery has some advantages over an orbit construction, though. The sizes of Clifford groups are large and grow factorially with the matrix dimension, whereas extraspecial groups are rather small and easier to handle. An homomorphism to vector spaces over finite field can also be used to handle the construction, which generates results on the sizes of the achievable codes and their minimum distances. Using the orthoplex bound for the complex Grassmannian, and some of the codes are shown to be optimum

complex packings, some codes reach the bound with the maximum number of points.

By using a subset of the codewords, smaller packings satisfying the equal-power per-antenna constraint can be constructed. Some of the constructions are shown to satisfy this constraint in an optimal manner using a modification of the Conway-Hardin-Sloane spherical embedding of the Grassmannian for equal-power per-antenna codebooks.

An example of resulting codebook for four transmit antennas with 1- and 2-stream transmissions is given in Table 5.4. The codebook splits to three parts. Codebook A corresponds to antenna subset selection. Codebook {B, C} satisfies the equal-power per-antenna constraint for 2-stream transmission, while codebook C satisfies the equal power per-antenna constraint for both 1-stream and 2-stream transmissions. In Table 5.4, codebooks are not normalized.

Results related to extraspecial code constructions from  $n_t = 2$  to  $n_t = 9$  (excluding  $n_t = 6$  since it is not a power of a prime) are displayed in Table 5.5. Optimality of the code is shown by reaching the orthoplex bound, codes satisfying the equal power per-antenna constraint are commented as “EP”, optimality with reference to this constraint is shown by reaching the corresponding orthoplex bound. For  $n_t = 4$ , the codes can be found in Table 5.4. For the cases  $n_t = n_s$ , the codes consists of unitary matrices belonging to a maximal set of mutually unbiased bases (MS-MUB), see e.g. [27] for details.

**Table 5.4.** Codebooks from extraspecial-group framework for 4 transmit antennas.

A	$\begin{bmatrix} 1 & 0 & 0 & 0 \\ 0 & 0 & 1 & 0 \\ 0 & 0 & 0 & 1 \\ 0 & 1 & 0 & 0 \end{bmatrix}$	$\begin{bmatrix} 1 & 1 & 0 & 0 \\ -i & i & 0 & 0 \\ 0 & 0 & 1 & 1 \\ 0 & 0 & -i & i \end{bmatrix}$	$\begin{bmatrix} 1 & 1 & 0 & 0 \\ 0 & 0 & 1 & 1 \\ i & -i & 0 & 0 \\ 0 & 0 & -i & i \end{bmatrix}$
B	$\begin{bmatrix} 1 & 0 & 0 & 1 \\ 1 & 0 & 0 & -1 \\ 0 & -1 & 1 & 0 \\ 0 & 1 & 1 & 0 \end{bmatrix}$	$\begin{bmatrix} 1 & 0 & 0 & 1 \\ 0 & -1 & 1 & 0 \\ 1 & 0 & 0 & -1 \\ 0 & 1 & 1 & 0 \end{bmatrix}$	$\begin{bmatrix} 1 & 0 & 1 & 0 \\ 0 & 1 & 0 & 1 \\ 0 & 1 & 0 & -1 \\ 1 & 0 & -1 & 0 \end{bmatrix}$
C	$\begin{bmatrix} 1 & 1 & 1 & 1 \\ 1 & 1 & -1 & -1 \\ 1 & -1 & 1 & -1 \\ 1 & -1 & -1 & 1 \end{bmatrix}$	$\begin{bmatrix} 1 & 1 & 1 & 1 \\ 1 & -1 & 1 & -1 \\ -i & -i & i & i \\ -i & i & i & -i \end{bmatrix}$	$\begin{bmatrix} 1 & 1 & 1 & 1 \\ -i & i & -i & i \\ 1 & 1 & -1 & -1 \\ -i & i & i & -i \end{bmatrix}$
	$\begin{bmatrix} 1 & 1 & 1 & 1 \\ -i & -i & i & i \\ -i & i & -i & i \\ 1 & -1 & -1 & 1 \end{bmatrix}$	$\begin{bmatrix} 1 & 1 & 1 & 1 \\ -i & i & i & -i \\ 1 & -1 & 1 & -1 \\ i & i & -i & -i \end{bmatrix}$	$\begin{bmatrix} 1 & 1 & 1 & 1 \\ 1 & -1 & -1 & 1 \\ 1 & -1 & 1 & -1 \\ -1 & -1 & 1 & 1 \end{bmatrix}$

**Table 5.5.** Example of codes from the extraspecial-group framework. Cardinality is  $n_{cb}$  and minimum squared distance  $\delta_c^2$ . For  $n_t \neq n_s$ ,  $\delta_c$  corresponds to the minimum Grassmann distance  $\delta_g$ . For  $n_t = n_s$ ,  $\delta_c$  corresponds to the minimum permutation-invariant flag distance  $\delta_p$ .

$n_t$	$n_s$	$n_{cb}$	$\delta_c^2$	Comments
2	1	4	$\frac{1}{2}$	EP optimum
2	1	6	$\frac{1}{2}$	Optimum
2	2	2	1	EP for any sub-rank
2	2	3	1	MS-MUB
3	1	9	$\frac{2}{3}$	EP Optimum
3	1	12	$\frac{2}{3}$	Optimum
3	3	3	2	EP for any sub-rank
3	3	4	2	MS-MUB
4	1	32	$\frac{1}{2}$	EP / columns of {C}
4	1	60	$\frac{1}{2}$	Columns of {A, B, C}
4	2	16	1	EP optimum/ EP for sub-rank / $4 \times 2$ matrices in {C}
4	2	24	1	EP optimum / $4 \times 2$ matrices in {B, C}
4	2	30	1	Optimum / $4 \times 2$ matrices in {A, B, C}
4	4	8	2	EP for any sub-rank / $4 \times 4$ matrices in {C}
4	4	15	2	3 MS-MUB / $4 \times 4$ matrices in {A, B, C}
5	1	25	0.8	EP optimum
5	1	30	0.8	Optimum
5	5	5	4	EP for any sub-rank
5	5	6	4	MS-MUB
7	1	49	$\frac{6}{7}$	EP optimum
7	1	56	$\frac{6}{7}$	Optimum
7	7	7	6	EP for any sub-rank
7	7	8	6	MS-MUB
8	1	512	$\frac{1}{2}$	EP
8	1	1080	$\frac{1}{2}$	EP
8	2	896	1	EP
8	2	1260	1	EP
8	4	112	2	EP optimum
8	4	126	2	Optimum
8	8	64	4	EP for any sub-rank
8	8	135	4	15 MS-MUB
9	1	243	$\frac{2}{3}$	EP
9	1	360	$\frac{2}{3}$	EP
9	3	108	2	EP optimum
9	3	120	2	Optimum
9	9	27	6	EP for any sub-rank
9	9	40	6	4 MS-MUB

### 5.3 Expansion to Stiefel Codes

Here, we consider Stiefel orbit codes arising from the linear representation of the projective groups considered in the previous sections. The codes are expansions of Grassmann orbit codes as direct products of a Grassmannian code and a unitary code. Indeed, the obtained codes are more than just a central extension of the Grassmann code. The codes obtained are extensions of Grassmannian codes by a finite group of right unitary rotations. Non-trivial stabilizers are only possible if some non-trivial group elements have eigenvalue 1. Otherwise, the size of the codebook is of the size of the linear group considered.

In Publication VI, we give examples of Stiefel codes arising from the Grassmann codes of Publication V. Their cardinality and minimum distance are summarized in Table 5.6, where  $N_g$  and  $\delta_g$  stand for the cardinality and minimum distance in the Grassmann manifold, whereas  $N_s$  and  $\delta_s$  stand for the cardinality and minimum distance in the Stiefel manifold. Their Stiefel squared minimum distances are evaluated in percentage of the Hamming-type bound (3.20).

The Stiefel manifold  $\mathcal{V}_{2,1}^{\mathbb{C}}$  is isomorphic to the 3-sphere, and these two spaces can be easily mapped to each other. Codes described for  $\mathcal{V}_{2,1}^{\mathbb{C}}$  are thus not new and are only interesting as tutorial examples. Some of the codes are optimal. An orbit of  $D_8$  gives an optimal  $(8, 2)$ -orthoplex Stiefel code. An orbit of  $S_3$  leads to an example of optimal joint Grassmannian-Stiefel packings with cardinality 3, meeting the simplex bounds for both manifolds. The Stiefel orbit of  $S_3$  of cardinality 6 and squared minimum distance 2 is a suborthoplex and is also optimal. Orbits from the binary tetrahedral group  $2T$  give an optimal Stiefel  $(24, 1)$ -packing, vertices of the 24-cell. This is a well-known polyhedron in 4D with well-understood symmetry, and known to lead to an optimal packing [84]. Orbits from the binary octahedral group  $2O$  lead to a codebook of 48 points on the Stiefel manifold with squared minimum distance  $2 - \sqrt{2} \approx 0.59$ , a combination of the 24-cell and its dual which is also a 24-cell. For comparison, the best known packing of this size has a squared minimum distance of  $\approx 0.62$  [84].

Using the central extension  $2C2$  of the Clifford group in 4D, we describe some codes in  $\mathcal{V}_{4,1}^{\mathbb{C}}$  and  $\mathcal{V}_{4,2}^{\mathbb{C}}$ . In  $\mathcal{V}_{4,1}^{\mathbb{C}}$ , the orbit of a  $(60, 0.5)$ - Grassmann code expands to a  $(480, 2-\sqrt{2})$ - Stiefel code. The orbit of a  $(480, \frac{3}{16})$ - Grassmann code expands to a  $(3840, 2-\frac{5}{2\sqrt{2}})$ - Stiefel code. In  $\mathcal{V}_{4,2}^{\mathbb{C}}$ , the optimum Grassmann orthoplex orbit generates an extension to a  $(5760, 4-2\sqrt{2})$ - Stiefel

code. The 320-, 360-, and 1440- Grassmann orbit lead to a  $(15360, 4-2\sqrt{2})$ -,  $(23040, 1)$ -, and  $(46080, 0.40)$ - Stiefel code, respectively. All these Stiefel codes are new.

**Table 5.6.** Some  $(N_s, \delta_s^2)$ -Stiefel orbit codes that are expansions of  $(N_g, \delta_g^2)$ -Grassmann orbit codes.

Dim	Group	Order	$N_g$	$\delta_g^2$	$N_s$	$\delta_s^2$	%HB	
$2 \times 1$	$D_8$	8	2	1	4	2	62	
			2	1	8	2	86	
			4	0.66	8	0.85	37	
	$S_3$	6	2	1	6	2	75	
			3	0.75	3	3	84	
			6	0.5	6	0.59	22	
	$D_{16}$	16	4	0.5	8	0.59	25	
			8	0.37	16	0.41	26	
	$2T$	24	4	0.66	24	1	81	
	$2O$	48	6	0.5	48	0.59	73	
	$4 \times 1$	$2C_2$	$2^6 6!$	60	0.5	480	0.59	32
				480	0.19	3840	0.23	21
$4 \times 2$	$2C_2$	$2^6 6!$	30	1	5760	1.17	41	
			320	0.44	15360	1.17	47	
			360	0.5	23040	1	43	
			1440	0.2	46080	0.4	19	



## 6. Joint Grassmann-Stiefel Codes for Product Codebooks

We consider a product codebook strategy where a single small codebook is implemented at the receiver to quantize larger MIMO channels, e.g. aggregate channels of cooperative MIMO base stations or point-to-point channels with large antenna configuration. This flexible method that reuses small point-to-point codebooks has many advantages. Only a single per-cell codebook needs to be stored for a fixed transmission rank, reducing design problems to smaller spaces which are typically easier to discretize. Large product codebooks naturally inherit some implementation properties from the per-cell codebook, e.g. input alphabet and transmit power per-antenna.

Focusing on the codebook design under this scenario, we propose a novel joint Grassmann-Stiefel codebook design aiming at good quantization of Grassmann and Stiefel manifolds with a single codebook, so that product codebook quantization becomes competitive with global Grassmann quantization. We present a vector quantizer to generate Stiefel codebooks conditioned on a fixed Grassmannian codebook. Some concrete examples of analytical joint Grassmann-Stiefel packings are also given. We finally discuss low-complexity codeword selection methods.

### 6.1 Product Codebook-Based Precoding

We follow the product codebook principle of [16] for feeding back CSI. This was proposed in order to accommodate to the possible dynamic number of cooperating BSs and to deal with heterogeneous path loss effects. Details on the considered CoMP channel model are in Chapter 2. A per-cell codebook  $\mathcal{C} = \{\mathbf{C}_1, \dots, \mathbf{C}_{n_{cb}}\}$  of  $(n_t \times n_s)$ -Stiefel matrices is shared between the transmitters and the receiver. This codebook is independent of the number of cooperating BSs, and large-scale path loss effects. The receiver



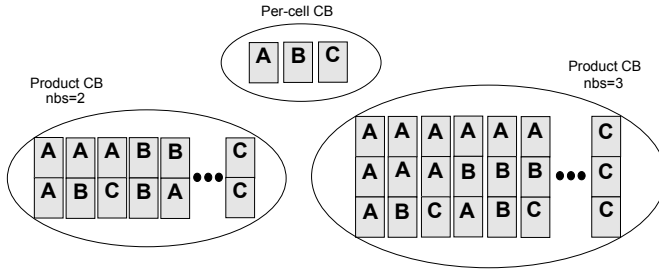


**Figure 6.1.** Illustration of product codebook principle for  $n_{bs} = 1, 2$  and  $3$ . Normalization is not shown.

quantizes  $\mathbf{V}_{ss}$  with a product codebook  $\mathcal{C}_{pr}$ . The product codebook is a Cartesian product of the per-cell codebook:  $\mathcal{C}_{pr} = \frac{1}{\sqrt{n_{bs}}} \mathcal{C} \otimes \cdots \otimes \mathcal{C}$ , i.e. a codeword in  $\mathcal{C}_{pr}$  is a normalized concatenation of  $n_{bs}$  single cell codewords. This is illustrated in Fig. 6.1. Finally, the receiver feeds back the set of indexes of the codewords of  $\mathcal{C}$  that form the selected product codeword.

Recall that with ML receiver, when considering the global  $(n_{bs} \times n_t) \times n_s$ -system, the performance of the product codebook is related to its interpretation as a discretization of the Grassmann manifold [23, 53, 56, 61]. While performance of the product codebook is invariant under right unitary rotations of the product codewords, the unitary invariance does not hold anymore for the per-cell codebook. The space of quantization is then the Grassmann manifold  $\mathcal{G}_{n_t, n_s}^{\mathbb{C}}$  for only one BS, and the Stiefel manifold  $\mathcal{V}_{n_t, n_s}^{\mathbb{C}}$  for the other  $(n_{bs} - 1)$ -BSs.

In Publication VII, we show that for a Haar distributed right singular space  $\mathbf{V}_{ss}$ , the optimum Stiefel quantization of a component of  $\mathbf{V}_{ss}$  is also Haar distributed. For the first BS,  $\mathcal{C}$  thus has to be a uniform Grassmannian codebook, whereas for the remaining BSs,  $\mathcal{C}$  also has to be a uniform Stiefel codebook. To construct uniform per-cell codebook, one can directly extend the standard Grassmann codebook criteria to the Stiefel manifold. In Publication VII, we motivate our choice of Stiefel distance by showing that the minimum Grassmann chordal distance of the product codebook  $\mathcal{C}_{pr}$  can be lower bounded by a function of the Grassmann and Stiefel chordal distances of the per-cell codebook  $\mathcal{C}$ :

$$\delta_g^2(\mathcal{C}_{pr}) \geq \min \left\{ \delta_g^2(\mathcal{C}), \frac{\delta_g^2(\mathcal{C}) + (n_{bs} - 1)\delta_s^2(\mathcal{C})}{n_{bs}^2} \right\}. \quad (6.1)$$

The proof is constructive and the bound is thus often tight.

Using a product codebook strategy results in two non-idealities.

i) A single-cell codebook designed to quantize the Grassmann manifold

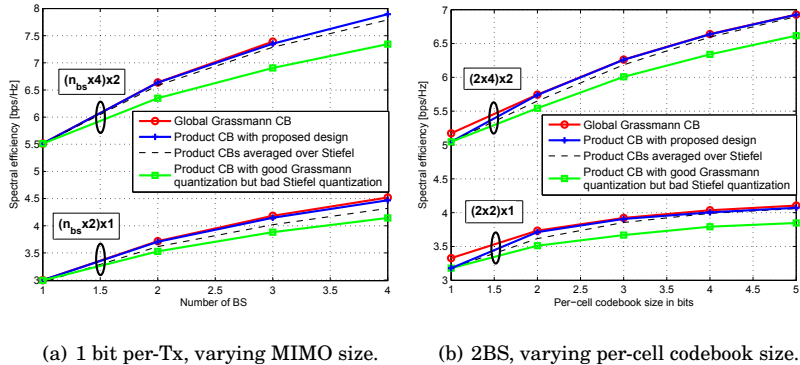


**Figure 6.2.** Performance comparison of product codebooks and global Grassmann codebooks at 10dB SNR.

$\mathcal{G}_{n_t, n_s}^C$  does not necessarily result in a good quantization of the Stiefel manifold  $\mathcal{V}_{n_t, n_s}^C$ .

ii) A residual loss would be also expected compared to a global codebook quantizing the larger Grassmannian  $\mathcal{G}_{n_{bs} n_t, n_s}^C$ , corresponding to the signal eigenspace of the receiver.

To make the performance of product codebook quantization close to optimal, we propose a novel joint Grassmann-Stiefel design of the per-cell codebook  $\mathcal{C}$ . An example of the achieved performance of such a design is illustrated in Fig. 6.2(a) and Fig. 6.2(b). Except when the per-cell codebook size is equal to one bit, the average performance of the proposed design is close to that of a global Grassmannian codebook (constructed here via Lloyd's algorithm). The gain of the proposed design is illustrated by comparison with a product codebook based on the same per-cell Grassmannian codebook but with (putatively) worst choice of Stiefel representatives. The mean performance of the Grassmann codebook averaged over all possible Stiefel representatives is also shown. The gap between the best and worst product codebook increase with increasing number of BSs, while relatively constant with increasing feedback bits. When the codebook size grows, product codebook performance averaged over Stiefel representatives is asymptotically reaching the performance of global codebook.

## 6.2 Joint Grassmann-Stiefel Codebooks

In order to have good per-cell codebooks that can be used in product codebooks as discussed above, we propose that a codebook is constructed by

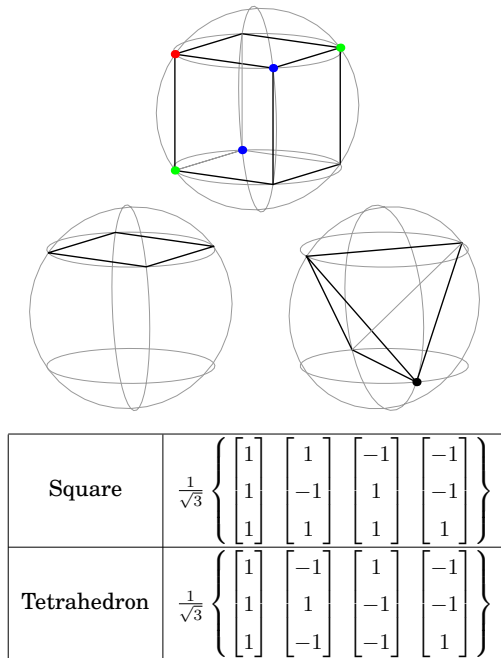


**Figure 6.3.** Joint Grassmannian-Stiefel codebook design in toy scenario of real codebook for 3 transmit antennas. On the upper graph the optimum 2-bit Grassmannian packing in  $\mathcal{G}_{3,1}^{\mathbb{R}}$ , a set of 4 antipodal points forming a cube. A Grassmannian codeword may be represented by any of the two points of same color, lying on a line through the origin. On the lower part, two alternatives of 2-bit Stiefel codebooks generating the above Grassmannian codebook: a square and a tetrahedron.

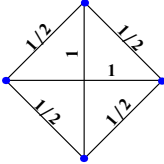
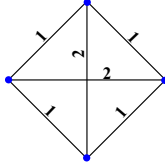
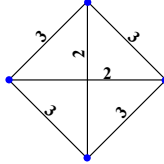
first designing a Grassmannian codebook according to standard criteria such as maximizing the minimum distance or minimizing an average distortion. Then, the representative in each Grassmannian plane in the codebook is chosen to optimize a metric on the Stiefel manifold. This means that we select a good Stiefel codebook conditioned on the codebook being simultaneously a good Grassmannian codebook.

The joint Grassmann-Stiefel codebook design problem is illustrated by the toy scenario of building a real codebook of four codewords for a transmission from 3 antennas in Fig 6.3. This leads to a rare example where visualization of the proposed approach is possible. The real Grassmannian  $\mathcal{G}_{3,1}^{\mathbb{R}}$  that needs to be discretized is the set of lines through the origin in the 3D Euclidean space. It can be understood as the set of antipodal points on the real unit sphere. The corresponding Stiefel manifold is the space of all 3D unit-norm vectors, and can be understood as the full sphere. A Grassmannian code is then a set of antipodal points, and choosing a rep-

**Table 6.1.** 2-bit *Square Codebook* for 2Tx antenna and a proposed modified version maximizing the average of the Stiefel distance between the codewords

Square CB	$\frac{1}{\sqrt{2}} \left\{ \begin{array}{c c c c} 1 & 1 & 1 & 1 \\ \hline 1 & -1 & i & -i \end{array} \right\}$
Stiefel-improved CB	$\frac{1}{\sqrt{2}} \left\{ \begin{array}{c c c c} 1 & 1 & -1 & -1 \\ \hline 1 & -1 & -i & i \end{array} \right\}$

Squared Grass. dist.	Squared Stief. dist.	
	Square CB	Stiefel-improved CB
		

representative for every Grassmannian codeword means simply choosing one of the two antipodal points on the sphere. A Stiefel-codebook, in turn, is a spherical code. The best four-codeword Grassmannian packing is found by taking the vertices of a cube – the eight vertices of the cube consist of four pairs of antipodal points, i.e. four Grassmannian lines. From this cube, there is four possible non-equivalent four-codeword spherical codes: for example by taking only points in the upper hemisphere we get a square, or by taking two points in both upper and lower hemispheres we get a tetrahedron. Those two alternative Stiefel codebooks generating the same Grassmannian code are given in Fig 4.3. The best Grassmann-Stiefel codebook is obtained by taking the vertices of the cube that form a tetrahedron. It turns out that the vertices of the tetrahedron gives actually the optimal 4-point spherical (Stiefel) codes under several criteria [69]. In this simple example, it is thus possible to have a codebook that is simultaneously an optimal Grassmannian and Stiefel packing.

This design can be applied to modify existing low-complexity codebooks from the literature. In Table 6.1, we give a Stiefel-improved version of the 2-bit *Square Codebook* discussed in Publications III and IV, which is related to the Mode 1 codebook of WCDMA [93] and the LTE codebook for 2-transmit antennas [51]. The modified version is obtained by only changing the sign of the third and last codeword. The squared Stiefel distances between the codewords of the proposed codebook are either 2 or 3, while for the original codebook they were either 1 or 2. This codebook has been

found by brute-force search over QPSK alphabet for the three last code-words. Furthermore, simulations over all possible phases suggest that this is putatively the best codebook conditioned on the original codebook maximizing the  $p$ -mean Stiefel distance for  $p = 1, 2, -1$  and  $-2$ .

### 6.3 Lloyd-type Algorithm for Joint Grassmann-Stiefel Codebook

A Lloyd-type algorithm to generate a low-distortion Stiefel codebook conditioned on a Grassmann codebook is presented in Publication VII.

The algorithm is a non-trivial generalization of Lloyd's algorithm, where a centroid at a given iteration, used to construct a Voronoi cell, is not necessarily the one updated to the new centroid of the cell. In each Voronoi cell of the Stiefel manifold, the original codeword is not replaced by the computed centroid. Instead, the algorithm is looking for the closest codeword to the the centroid using Grassmann distance rather than Stiefel distance. As a result, for each Voronoi cell, the updated codeword is not necessarily belonging to the original Voronoi cell. Then the selected codeword is replaced by the Stiefel representative in its Grassmann equivalence class closest to the centroid. Indeed, during a single iteration some codewords can be updated several times and some others not at all. This occurs in particular in the first iterations. This phenomenon is related to the non-trivial embedding of the Grassmannian to the Stiefel manifold, and is crucial for convergence. Simulation results show that the proposed algorithm converges well.

This feature is illustrated in Fig 6.4 for a toy scenario of choosing the Stiefel representative of a real Grassmann codebook in  $\mathcal{G}_{2,1}^{\mathbb{R}}$ . The Stiefel manifold in this case is the unit circle  $S^1$ , and the Grassmannian is the set of lines through the origin in 2D, or pairs of antipodal points on a circle. At Step 1) , the Stiefel representatives of the three Grassmannian lines have been given in the right half circle. In Steps 2) and 3), the algorithm generates a random source and partitions the Stiefel manifold based on a nearest neighbor rule. The Stiefel Voronoi cells corresponding to these codewords are depicted in blue, red and orange. Non-trivial differences as compared to the conventional Lloyd's algorithm can be seen in Step 4) where the algorithm sequentially computes a centroid and updates a codeword. The centroid of the orange Voronoi cell is depicted in a). It happens to be closer to the red Grassmannian line than to the orange one as depicted in b). Thus in c)-d) we update the Stiefel representative

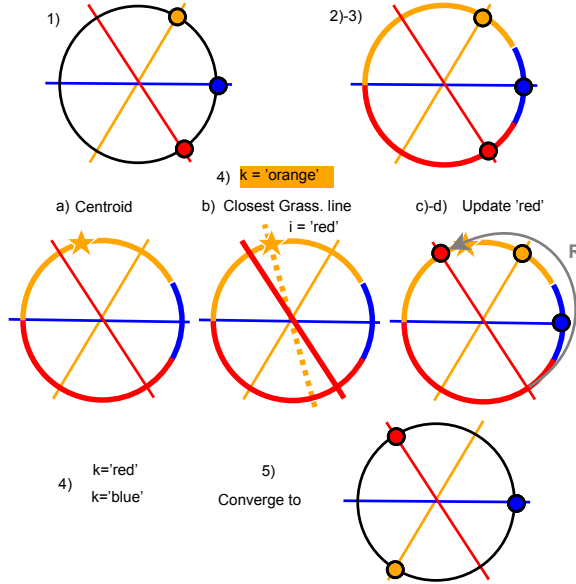


**Figure 6.4.** Illustration of the Lloyd-type algorithm for a real Stiefel codebook in  $\mathcal{V}_{2,1}^{\mathbb{R}} \cong S^1$  conditioned on a real Grassmannian codebook in  $\mathcal{G}_{2,1}^{\mathbb{R}}$ .

of the red line to this centroid, not the representative of the orange line. Next, if we consider the centroid of the red Voronoi region, we update the representative of the orange line, whereas the centroid of the blue region leads to the representative of the blue line being fixed. As a consequence, we have found the optimum three-element Grassmann-Stiefel packing in 5).

## 6.4 Codeword Selections

For a given codebook, optimum quantization of the  $n_{bs}n_t \times n_s$  channel eigenspace requires exhaustive search over the codebook. Here, the product codebook has of cardinality  $n_{cb}^{n_{bs}}$ . This leads to exponential complexity w.r.t the number of BSs  $\mathcal{O}(n_{cb}^{n_{bs}})$ . Complexity can be reduced from  $\mathcal{O}(n_{cb}^{n_{bs}})$  to  $\mathcal{O}(n_{bs}n_{cb})$  by selecting per-cell components rather than selecting jointly the product codeword [16, 86]. In [16], a lower-complexity selection algorithm trading performance against complexity is proposed, based on two successive exhaustive searches of size  $n_{bs}n_{cb}$  and  $k^{n_{bs}}$ , where  $k$  is the cardinality of preselected per-cell sub-codebooks. Independent and serial selection are proposed for single-stream beamforming in [42, 86].

In Publication VII, we discuss five different codeword selection principles for multi-stream product codebooks. Two joint selection methods of

complexity  $\mathcal{O}(n_{cb}^{n_{bs}})$  are considered, followed by three selections of complexity  $\mathcal{O}(n_{bs}n_{cb})$ .

- *Joint codeword selection* is done by selecting the product codeword that minimizes the global Grassmann distance to  $\mathbf{V}_{ss}$  [16]. The complexity is  $\mathcal{O}(n_{cb}^{n_{bs}})$ .
- *Joint codeword selection with transformed codebook* improved the previous selection method in case of path loss imbalance [86] by borrowing the idea of transformed codebooks for spatially correlated channel [54]. The complexity remains  $\mathcal{O}(n_{cb}^{n_{bs}})$ .
- *Independent Grassmann codeword selection* was an alternative proposed in [86]. Here, each single cell channel component matrix is quantized independently using the Grassmann chordal distance. This method leads to a loss of performance as it does not take into account the phase ambiguity between the components of the optimum precoding vector as recognized in [86], or the more general unitary matrix ambiguity. The complexity is reduced to  $\mathcal{O}(n_{bs}n_{cb})$ .
- *Independent Grassmann-Stiefel codeword selection*: In order to quantize the per-cell channel components independently and efficiently, the unitary matrix ambiguity between the different channels should be taken into account. We suggest that first the strongest channel is quantized using the Grassmannian distance. Then the unitary rotation  $\mathbf{R}$  not seen by this Grassmannian codeword selection can be found by performing a polar decomposition. The channels from the other BSs, with the rotation  $\mathbf{R}$  taken into account, are then quantized using the Stiefel distance. Complexity is  $\mathcal{O}(n_{bs}n_{cb})$ .
- *Serial Codeword selection*: This method borrows the main idea of serial selection from [42], adapted here to perform codeword selection with a transformed codebook in a sequential manner. The strongest channel is first quantized as in the previous independent selection method. Then the per-cell components are selected sequentially taking into account the large-scale channel components. Complexity is  $\mathcal{O}(n_{bs}n_{cb})$ .

Figure 6.5 depicts the variation of performance when the large scale

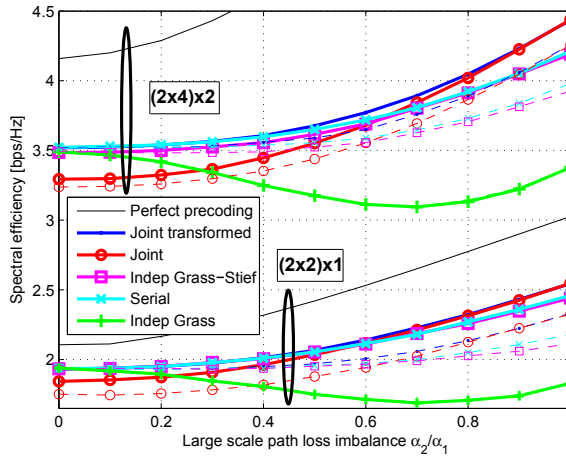


**Figure 6.5.** Spectral efficiency of  $4 \times 1$  and  $8 \times 2$  systems using  $2 \times 1$  and  $4 \times 2$  codebooks respectively, as a function of large scale path gains imbalance. The strongest channel is fixed at a SNR of 6 dB. Codebooks with one feedback bit per transmit antenna. The legend indicates the codeword selection methods. Performance of original codebooks is represented in dashed lines, while for Stiefel-improved versions, in solid lines.

path gain for the first and the second BS are different. The lower curves represent 2 cooperative BSs with 2 Tx antennas with 2-bit Square Codebook and its Stiefel-improved version of Table 6.1. The upper curves represent two 4-antenna BSs serving a 2 antenna user with 4-bit C-Codebook from Publication IV and Stiefel-improved version by the proposed Lloyd-type algorithm. The graph can be interpreted as the performance depending of the position of the user, from the center of the cell to the cell edge.

The Stiefel-improved codebooks lead to better performance for all codeword selection methods except independent selection with Grassmann distance. Using the Stiefel distance consequently improves performance of independent selection. The serial selection offers slightly better performance than independent Grassmannian-Stiefel selection. Both the independent Grassmannian-Stiefel selection and the serial selection perform close to joint selection. The performance gap between joint selection and independent and serial selection first reduces and then is reversed when the large scale path gain imbalance grows. With imbalance, joint selection is not optimal anymore as it quantizes the channel components with equal weight. Transforming the codebook cures this problem, and gives the overall best selection method: matching the performance of independent selections for large imbalance and joint selection for no imbalance.





## 7. Flag Codebooks for MIMO Systems with Linear Receiver

In point-to-point communications with maximum likelihood (ML) receiver, the performance of a unitary precoding codebook depends on the distance properties of the Grassmannian planes generated by the codebook. This has led to the well-known Grassmannian codebook design [55] where the codebook is understood as a discretization of the Grassmann manifold. While Grassmann precoding has attracted much attention, other transmission scenarios or constraints may lead to the need to design codebooks in other flag manifolds.

We illustrate this by focusing on precoding for MIMO systems with a linear receiver, such as a zero-forcing (ZF) or minimum mean square (MMSE) receivers. With a linear receiver, the Grassmannian precoding design used for ML receivers is not anymore appropriate [57]. In Publication VIII, the spaces of interest are shown to be simple permutation-invariant flag manifolds.

Of specific interest is the case when the number of streams, and the number of receive and transmit antennas are the same. In this set up, the corresponding Grassmannian collapses to a single point making Grassmannian precoding irrelevant. Accordingly, precoding does not improve the information rate with ML receiver. On the other hand, with linear receiver, gain may be obtained from precoding using the proposed flag codebook design. Simulations show that this gain is relatively small when only few feedback bits are used for more than two transmit antennas. This differs from the behavior of low-rank transmission, where it is known that a small number of feedback bits can allow near optimal channel adaptation.

## 7.1 Achievable Information Rates

Let the singular values of  $\mathbf{H}$  be  $\sigma_1^{1/2} \geq \dots \geq \sigma_{n_m}^{1/2}$  with  $n_m = \min(n_r, n_t)$ . For a fixed precoding vector  $\mathbf{W} \in \mathbb{C}^{n_t \times n_s}$ , the achievable rate depends on the receiver type. Denote the singular values of the effective channel  $\mathbf{H}_{\text{eff}} = \mathbf{H}\mathbf{W}$  by  $\lambda_1^{1/2} \geq \dots \geq \lambda_{n_s}^{1/2}$ .

*Maximum Rate:* Without water-filling and for a given transmission rank constraint  $n_s$ , the maximum achievable rate of the system is [23, 87]

$$I_{n_s} = \sum_{k=1}^{n_s} \log_2(1 + \gamma \sigma_k) \leq \log_2 \det(\mathbf{I} + \gamma \mathbf{H}\mathbf{H}^H) = I_{n_m} \quad (7.1)$$

where  $I_{n_m}$  is the maximum achievable rate without transmission rank constraint.

*ML receiver:* With maximum likelihood receiver the achievable rate with precoding  $\mathbf{W}$  is

$$I_{\text{ml}}(\mathbf{W}) = \log_2 \det(\mathbf{I} + \gamma \mathbf{H}_{\text{eff}} \mathbf{H}_{\text{eff}}^H) = \sum_{k=1}^{n_s} \log_2(1 + \gamma \lambda_k). \quad (7.2)$$

We have  $I_{\text{ml}}(\mathbf{W}) \leq I_{n_s}$ . The latter is achievable with  $\mathbf{W}_{\text{opt}} = \mathbf{V}_{n_s}$  [23] where  $\mathbf{V}_{n_s} \in \mathbb{C}^{n_t \times n_s}$  is a matrix composed by the right singular vectors of  $\mathbf{H}$  corresponding to its  $n_s$ -largest singular values.

*Linear receiver:* The receiver employs a linear receiver of the form  $\mathbf{F}\mathbf{H}_{\text{eff}}^H$ , where  $\mathbf{F} = (\gamma \mathbf{H}_{\text{eff}}^H \mathbf{H}_{\text{eff}} + a \mathbf{I}_{n_s})^{-1}$ . With  $a = 0, 1$ , we get a ZF and MMSE receiver, respectively. The corresponding rate is [39]

$$I_{\text{lr}}(\mathbf{W}) = \sum_{k=1}^{n_s} \log_2(1 + \gamma_k), \quad (7.3)$$

where  $\gamma_k = (\mathbf{F}_{k,k})^{-1} - a$  is the post-processing SINR of the  $k$ -th data stream. In general we have  $I_{\text{lr}}(\mathbf{W}) \leq I_{\text{ml}}(\mathbf{W})$ . In [57] it is shown that there exists a unitary matrix  $\mathbf{U} \in \mathcal{U}_{n_s}$  such that  $I_{\text{lr}}(\mathbf{W}\mathbf{U}) = I_{\text{ml}}(\mathbf{W})$  and a precoder partitioning is proposed accordingly. As for ML receiver, an optimum precoding matrix is given by  $\mathbf{W}_{\text{opt}} = \mathbf{V}_{n_s}$ .

## 7.2 Linear Receiver versus ML Receiver

The following difference between linear and ML receivers should be stressed:

**1) Full rank  $n$ -by- $n$  MIMO:** For  $n_s = n_t = n_r$ , we have  $I_{\text{ml}}(\mathbf{W}) = I_{n_m}$  for any  $\mathbf{W} \in \mathcal{U}_{n_t}$  and thus unitary precoding does not change the transmission rate with ML receiver. With a linear receiver, the rate is a function of the precoding matrix, and  $I_{\text{lr}}(\mathbf{W}) \leq I_{n_m}$ .

**2) Space of non-equivalent precoder:** Let  $\sim$  be the equivalence relation declaring two precoding matrices equivalent, so that  $\mathbf{W}_1 \sim \mathbf{W}_2$ , if and only if  $I(\mathbf{W}_1) = I(\mathbf{W}_2)$ .

*ML receiver:* The information rate is invariant under any right-unitary rotations of the precoding codeword:  $I_{\text{ml}}(\mathbf{W}\mathbf{U}) = I_{\text{ml}}(\mathbf{W})$  for any  $\mathbf{U} \in \mathcal{U}_{n_s}$ . The set of equivalence classes of precoding matrices is exactly the Grassmann manifold  $\mathcal{G}_{n_t, n_s}^{\mathbb{C}}$ .

*Linear receiver:* The statement above does not hold anymore. The information rate with linear receiver (7.3) is invariant under permutations and phase multiplications of columns of the precoding matrix,  $I_{\text{lr}}(\mathbf{W}\mathbf{D}\mathbf{P}) = I_{\text{lr}}(\mathbf{W})$ , for any permutation matrix  $\mathbf{P} \in \mathcal{U}_{n_s}$  and any diagonal matrix  $\mathbf{D} \in \mathcal{U}_{n_s}$ . The set of equivalence classes of precoding matrices is thus the permutation-invariant flag manifold  $\tilde{\mathcal{F}}_{n_t, n_s}^{\mathbb{C}}$ .

### 7.3 Codebook Designs

Now we assume that the channel matrix is a random variable and that the transmitter picks the precoding matrix from a codebook  $\mathcal{C}$  following a quantization rule. Given the instantaneous transmission rate  $I(\mathbf{H}, \mathbf{W})$  of a precoding matrix  $\mathbf{W}$ , the average information rate is

$$\bar{I} = \mathbb{E}_{\mathbf{H}} [I(\mathbf{H}, \mathbf{C}_{\mathbf{q}(\mathbf{H})})]. \quad (7.4)$$

The codebook should be designed as a discretization of the space  $\mathcal{V}_{n_t, n_s}^{\mathbb{C}} / \sim$  of equivalence classes of precoding matrices. The task thus becomes:

**ML receiver:** discretize the Grassmann manifold  $\mathcal{G}_{n_t, n_s}^{\mathbb{C}}$ ,

**Linear receiver:** discretize the flag manifold  $\tilde{\mathcal{F}}_{n_t, n_s}^{\mathbb{C}}$ .

An optimum quantization  $\mathbf{q}^*(\mathbf{H}) = \arg \max_{1 \leq i \leq n_b} I(\mathbf{C}_i)$  is untractable. For Grassmannian precoding, quantization with Grassmann chordal distance,  $\mathbf{q}_g(\mathbf{V}_{n_s}) = \arg \min_{1 \leq i \leq n_b} d_g(\mathbf{V}_{n_s}, \mathbf{C}_i)$ , has been considered instead and shown to be asymptotically optimum [23]. Corresponding good codebooks are thus designed by minimizing the average squared distortion  $\mathbb{E}[d_g^2(\mathbf{V}_{n_s}, \mathbf{C}_{\mathbf{q}_g(\mathbf{V}_{n_s})})]$  [22, 23]. We extend this principle to codebook design on the flag manifold by replacing the chordal distance  $d_g$  by the distance  $d_p$  defined in (3.11). A corresponding Lloyd's algorithm providing low-distortion codebooks is given in Publication VIII.

## 7.4 Simulations

We illustrate by simulations the performance of the proposed design for i.i.d Rayleigh channels, using codebooks generated by the Lloyd's algorithm described in Publication VIII and the flag orbit codes of Chapter 5. While the codebooks has been designed using the distance metric  $d_p$ , we use the optimal quantization metric, i.e. the information rate, for selection of the codeword at the receiver. Indeed, unlike for the Grassmann precoding where optimal selection and chordal distance selection show similar performance, codeword selection on flag manifold with  $d_p$  injures a significant performance loss.

Fig. 7.1 shows the information rate for  $4 \times 2$  MIMO systems with ZF receiver, rank-2 transmission and 4-bit codebooks in  $\tilde{\mathcal{F}}_{4,2}^C$  and  $\mathcal{G}_{4,2}^C$ . The flag manifold codebook outperforms the Grassmannian with more than 1 dB. The performance of the precoding partitioning scheme of [57] is also depicted. Its performance falls between the Grassmannian and flag codebooks. In the partitioning, bits are split equally between Grassmannian precoding and 2-stream orthogonalization, and codebooks for both are generated by Lloyd's algorithms.

Fig. 7.2 shows the information rate for a full-rank system with an equal number of transmit and receive antennas. Additionally to codebooks from Lloyd's algorithm, simulations are performed with flag orbit codes of Chapter 5. The size of the codes is expressed in bits. In this scenario, as pointed above, precoding is irrelevant if ML receiver is used, while for a linear re-

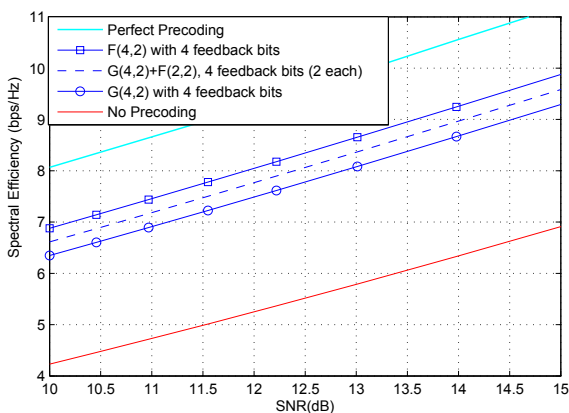
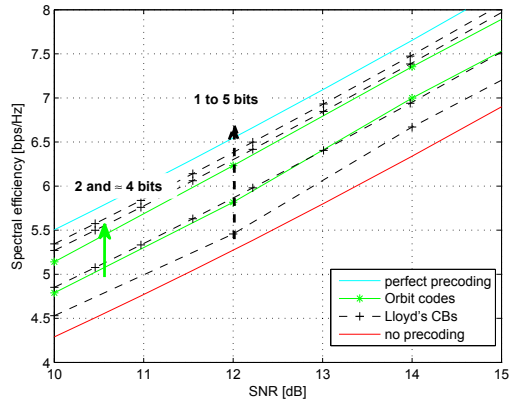


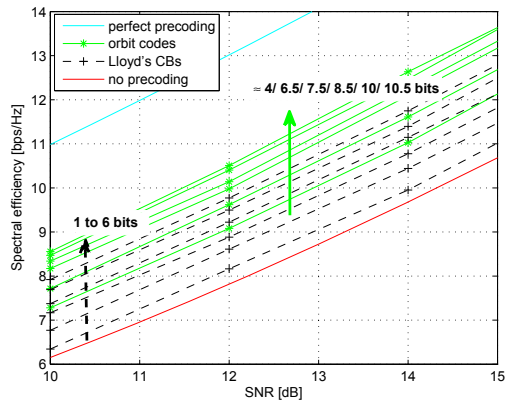
**Figure 7.1.** Information rate with ZF receiver for  $n_t = 4$ ,  $n_r = n_s = 2$ , four-bit ( $n_b = 16$ ) codebooks designed in flag  $\tilde{\mathcal{F}}_{4,2}^C$  and Grassmann  $\mathcal{G}_{4,2}^C$  manifolds, and precoding partitioning [57] with 2 bits for Grassmannian and orthogonalization each.

ceiver, precoding has an effect. For  $2 \times 2$  systems, it is possible to recover most of the gap between no precoding and perfect precoding with a few feedback bits. However, when the number of antennas increases, e.g. for  $n_t = n_r = 4$  in Fig. 7.2, the marginal gain for a small number of bits is small. In the SNR range depicted, the performance gap between no and perfect precoding is some 5dB. Precoding with 10 bits recovers only half of this gap. The codebooks from Lloyd's algorithm perform slightly better than the orbit code.

The curves on Fig. 2 of Publication VIII correspond to performance with codeword selection using the flag chordal distance. Thus, in Publication VIII the performance is lower compared to Fig. 7.2 where optimum selection is performed.



(a) Full rank transmission of  $2 \times 2$ . Codebooks size up to 5 bits.



(b) Full rank transmission of  $4 \times 4$ . Codebooks size up to 10 bits.

**Figure 7.2.** Information rate of full rank transmission  $n_t = n_r = n_s$  with ZF receiver.



## 8. Conclusions

Motivated by applications to codebook-based unitary precoding for limited-feedback MIMO systems, we have considered coding in flag manifolds equipped with chordal distances. Codebook-based unitary precoding is widely employed, and several codebook designs in the literature are examples of flag manifold discretization. Analytical constructions are considered to acquire analytical control of the codebooks, so that e.g. providing low implementation-complexity for practical systems.

We described spherical embeddings of flag manifolds with the corresponding chordal distances. Flag codes are a subclass of spherical codes, and coding and geometrical problems on flag manifolds are mathematical problems of independent interest. We have discussed centroid computation, volume of metric balls, and Hamming-type bounds on Grassmann and Stiefel codes with chordal distance. Geometry of manifolds depends on the choice of the Riemannian metric, implying an Euclidean embedding. With a chordal distance, understanding the corresponding embedding enables leveraging results from Euclidean geometry literature.

Code constructions are based on geometric intuition from the lowest dimensional flag manifolds, the circle and the real sphere. We have discussed the problem of designing closed-form codebooks for two transmit antennas. The problem reduces to a quantization problem on a real 2-sphere. Utilizing a simple isomorphism, we were able to derive simple closed form codebooks from spherical arrangements with inherent low implementation complexity. The discussed code construction is specific for two transmit antenna systems and cannot be straightforwardly generalized to higher dimensions.

For more transmit antennas, i.e. higher dimensional codebooks, we consider three different constructions: orbit codes, extraspecial group constructions, and product codebooks.



We discussed flag orbit codes arising from projective unitary group representations. We described few examples in 2D and 4D for the Grassmann manifold and unitary matrices modulo column permutations and column-wise rotations. We also described Stiefel orbit codes, as group expansions of constructed Grassmann orbit codes. For dimensions equal to a power of a prime, we have presented a construction of Grassmannian packings related to representation theory of extraspecial groups. We prove the optimality of several of the constructed codebooks with reference to an equal-power per-antenna constraint. For MIMO precoding, orbit constructions enable building well structured codebooks. However, an orbit construction has the drawback of giving very little freedom in controlling the size of the codes, which often is not an exact number of bits. Also, for many antenna systems, this requires manipulating very large groups.

We have considered product codebook quantization where codewords from a single small point-to-point codebook are concatenated to quantize larger MIMO channels, e.g. channels from cooperative BSs. We have proposed a joint Grassmann-Stiefel codebook design to diminish the performance gap between product codebook quantization and global Grassmannian quantization. We have investigated methods to construct good Stiefel codebooks conditioned on Grassmannian codebooks. A Lloyd-type algorithm on Stiefel manifold conditioned on a given Grassmannian codebook is proposed, as well as some closed-form examples of joint Grassmann-Stiefel codebooks. For large MIMO system, product codebook framework is a promising method as it offers very good performance, and also reduces the codebook design to smaller spaces which are easier to handle.

We finally concentrated on the design of unitary codebooks for MIMO systems with linear receivers. The correct spaces of quantization are certain permutation-invariant flag manifolds. The pertinence of the design principle was illustrated by simulations. In full-rank MIMO with linear receiver, the capacity is not achieved by default unlike with ML receiver. Moreover, for more than two transmit antennas, precoding with limited feedback offers only small gain. Significant amounts of feedback bits are needed to improve the rates of high-rank MIMO transmission with linear receivers. This behavior differs significantly from low-rank unitary precoding whose success arises from good marginal gains for few feedback bits.

Possible directions for future research include extending the volume ball estimation, kissing radius and Hamming bound to other flag manifolds.

Using this volume estimation, it would be possible to generalize bounds on rate-distortion tradeoff in Grassmann manifolds [22] to Stiefel manifolds [49] and other flag manifolds. Then, distortion bounds may be used for evaluating the information rate of flag precoding. Accordingly, it would be interesting to quantify analytically the observation of Chapter 7 on the small marginal gain of precoding for full-rank MIMO with linear receiver. Alternatively, differential precoding could be investigated to cure this problem. Finally, another direction of future work is to build new orbit codes by investigating other finite groups.



# Bibliography

- [1] 3GPP TSG . RAN WG1 Meeting #55bis R1-090388, Ljubljana, Slovenia, 12-16 January, 2009.
- [2] V. Aggarwal, A. Ashikhmin, and A. Calderbank. A Grassmannian packing based on the nordstrom-robinson code. In *Proc. IEEE Inf. Theory Workshop*, pages 1–5, Oct. 2006.
- [3] A. Ashikhmin and A. Calderbank. Space-time Reed-Muller codes for non-coherent MIMO transmission. In *Proc. IEEE Int. Symp. Inf. Theory*, pages 1952–1956, Sept. 2005.
- [4] A. Ashikhmin and A. Calderbank. Grassmannian packings from operator reed-muller codes. *IEEE Trans. Inf. Theory*, 56(11):5689–5714, Nov. 2010.
- [5] A. Ashikhmin, A. Calderbank, and W. Kewlin. Multidimensional second order Reed-Muller codes as Grassmannian packings. In *Proc. IEEE Int. Symp. Inf. Theory*, pages 1001–1005, July 2006.
- [6] A. Ashikhmin and R. Gopalan. Grassmannian packings for efficient quantization in MIMO broadcast systems. In *Proc. IEEE Int. Symp. Inf. Theory*, pages 1811–1815, June 2007.
- [7] C. Bachoc. Linear programming bounds for codes in Grassmannian spaces. *IEEE Trans. Inf. Theory*, 52(5):2111–2125, May 2006.
- [8] C. Bachoc, Y. Ben-Haim, and S. Litsyn. Bounds for codes in products of spaces, Grassmann, and Stiefel manifolds. *IEEE Trans. Inf. Theory*, 54(3):1024–1035, Mar. 2008.
- [9] A. Barg and D. Nogin. Bounds on packings of spheres in the Grassmann manifold. *IEEE Trans. Inf. Theory*, 48(9):2450 – 2454, Sep. 2002.
- [10] A. Barg and D. Nogin. A bound on Grassmannian codes. In *Proc. IEEE Int. Symp. Inf. Theory*, pages 997–1000, July 2006.
- [11] A. Borel. Groupes algébriques. *Séminaire N. Bourbaki*, 3(121):1–10, 1954-1956.
- [12] R. Bott and L. Tu. *Differential forms in algebraic topology*. Springer – Verlag, 1982.
- [13] M. Bowick, C. Cecka, L. Giomi, A. Middleton, and K. Zielnicki. Thomson Problem @S.U. published electronically at <http://physics.syr.edu/condensedmatter/thomson/thomson.htm>.

- [14] A. Calderbank, P. Cameron, W. Kantor, and J. Seidel. Z4-Kerdock codes, orthogonal spreads, and extremal Euclidean line-sets. *Proc. London Math. Soc.*, 75(2):436–480, 1997.
- [15] A. Calderbank, R. Hardin, E. Rains, P. Shor, and N. Sloane. A group-theoretic framework for the construction of packings in Grassmannian spaces. *J. Algebraic Combin.*, 9:129–140, 1999.
- [16] Y. Cheng, V. Lau, and Y. Long. A scalable limited feedback design for network MIMO using per-cell product codebook. *IEEE Trans. Wireless Commun.*, 9(10):3093–3099, Oct. 2010.
- [17] B. W. Clare and D. Kepert. The closest packing of equal circles on a sphere. *P. Roy. Soc. Lond. A Mat.*, 405(1829):329–344, 1986.
- [18] J. Conway, R. Hardin, and N. Sloane. Packing lines, planes, etc.: Packings in Grassmannian space. *Exp. Math.*, 5:139–159, 1996.
- [19] J. H. Conway and N. Sloane. *Sphere Packings, Lattices and Groups*. Springer-Verlag, New York, 2nd edition, 1993.
- [20] J. Creignou. Constructions of Grassmannian simplices. *eprint arXiv:cs/0703036*, Mar. 2007.
- [21] J. Creignou and H. Diet. Linear programming bounds for unitary space time codes. In *Proc. IEEE Int. Symp. Inf. Theory*, pages 1073–1077, July 2008.
- [22] W. Dai, Y. Liu, and B. Rider. Quantization bounds on Grassmann manifolds and applications to MIMO communications. *IEEE Trans. Inf. Theory*, 54(3):1108–1123, Mar. 2008.
- [23] W. Dai, Y. Liu, B. Rider, and V. Lau. On the information rate of MIMO systems with finite rate channel state feedback using beamforming and power on/off strategy. *IEEE Trans. Inf.*, 55(11):5032–5047, Nov. 2009.
- [24] I. Dhillon, R. Heath, T. Strohmer, and J. Tropp. Constructing packings in Grassmannian manifolds via alternating projection. *Exp. Math.*, 17(1):9–35, 2008.
- [25] P. Dragnev, D. Legg, and D. Townsend. Discrete logarithmic energy on the sphere. *Pacific J. Math.*, 207(2):345–358, 2002.
- [26] Q. Du, M. Gunzburger, and L. Ju. Constrained centroidal voronoi tessellations for surfaces. *SIAM J. Sci. Comput.*, 24(5):1488–1506, 2003.
- [27] T. Durt, B.-G. Englert, I. Bengtsson, and K. Życzkowski. On mutually unbiased bases. *Int. J. Quantum Inform.*, 8(04):535–640, 2010.
- [28] A. Edelman, T. Arias, and S. Smith. The geometry of algorithms with orthogonality constraints. *SIAM J. Matrix Anal. A.*, 20(2):303–353, 1998.
- [29] C. Ehresmann. Sur la topologie de certains espaces homogènes. *Ann. Math.*, 35(2):396–443, Apr. 1934.
- [30] T. Ericson and V. Zinoviev. *Codes on Euclidean Spheres*. North-Holland Mathematical Library, 2001.
- [31] K. Fan and A. Hoffman. Some metric inequalities in the space of matrices. *Proc. Amer. Math. Soc.*, 6(1):111–116, Feb. 1955.

- [32] G. Foschini and M. Gans. On limits of wireless communication in a fading environment when using multiple antennas. *Wireless Pers. Commun.*, 6(3):311–335, Mar. 1998.
- [33] R. Gray and D. Neuhoff. Quantization. *IEEE Trans. Inf. Theory*, 44(6):2325–2383, Oct. 1998.
- [34] G. Han and J. Rosenthal. Geometrical and numerical design of structured unitary space amp-time constellations. *IEEE Trans. Inf. Theory*, 52(8):3722–3735, 2006.
- [35] G. Han and J. Rosenthal. Geometrical and numerical design of structured unitary space-time constellations. *IEEE Trans. Inf. Theory*, 52(8):3722–3735, Aug. 2006.
- [36] G. Han and J. Rosenthal. Unitary space-time constellation analysis: An upper bound for the diversity. *IEEE Trans. Inf. Theory*, 52(10):4713–4721, Oct. 2006.
- [37] R. Hardin, N. Sloane, and W. Smith. Maximal volume spherical codes. published electronically at <http://www2.research.att.com/~njas/maxvolumes/>.
- [38] R. Hardin, N. Sloane, and W. Smith. Minimal energy arrangements of points on a sphere. published electronically at <http://www2.research.att.com/~njas/electrons/>.
- [39] R. Heath, S. Sandhu, and A. Paulraj. Antenna selection for spatial multiplexing systems with linear receivers. *IEEE Commun. Lett.*, 5(4):142–144, Apr. 2001.
- [40] O. Henkel. Sphere packing bounds in the Grassmann and Stiefel manifolds. *IEEE Trans. Inf. Theory*, 51:3445, Oct. 2005.
- [41] N. Higham. Matrix nearness problems and applications. In *Applications of Matrix Theory*, Oxford University Press, pages 1–27, 1989.
- [42] X. Hou and C. Yang. Codebook design and selection for multi-cell cooperative transmission limited feedback systems. In *Proc. IEEE Veh. Technol. Conf.*, pages 1–5, May 2011.
- [43] K. Huang, J. Andrews, and R. Heath. Performance of orthogonal beamforming for SDMA with limited feedback. *IEEE Trans. Veh. Technol.*, 58(1):152–164, Jan. 2009.
- [44] T. Inoue and R. Heath. Kerdock codes for limited feedback precoded MIMO systems. *Trans. Signal Process.*, 57(9):3711–3716, Sep. 2009.
- [45] A. T. James. Distributions of matrix variates and latent roots derived from normal samples. *Ann. Math. Statist.*, 35:475–501, June 1964.
- [46] M. Karakayali, G. Foschini, and R. Valenzuela. Network coordination for spectrally efficient communications in cellular systems. *IEEE Wireless Commun.*, 13(4):56–61, Aug. 2006.
- [47] I. Kim, S. Park, D. Love, and S. Kim. Improved multiuser MIMO unitary precoding using partial channel state information and insights from the Riemannian manifold. *IEEE Trans. Wireless Commun.*, 8(8):4014–4023, Aug. 2009.

- [48] J. Kim, W. Zirwas, and M. Haardt. Efficient feedback via subspace-based channel quantization for distributed cooperative antenna systems with temporally correlated channels. *EURASIP J. Adv. Sig. Pr.*, (847296):1–13, 2008.
- [49] R. Krishnamachari and M. Varanasi. Volume of geodesic balls in the complex Stiefel manifold. In *Proc. of Allerton Conf. on Comm. Cont. and Comp.*, pages 902–909, Sep. 2008.
- [50] R. Krishnamachari and M. Varanasi. Volume of geodesic balls in the real Stiefel manifold. In *Proc. 42nd Annu. Conf. Inf. Sci. Syst.*, pages 402–406, Mar. 2008.
- [51] P. Lee, J.-K. Han, and J. Zhang. MIMO technologies in 3GPP LTE and LTE-Advanced. *EURASIP J. Wirel. Commun. Netw.*, (302092):1–10, July 2009.
- [52] D. Love and R. Heath. Equal gain transmission in multiple-input multiple-output wireless systems. *IEEE Trans. on Commun.*, 51(7):1102–1110, 2003.
- [53] D. Love and R. Heath. Limited feedback unitary precoding for spatial multiplexing systems. *IEEE Trans. Inf.*, 51(8):2967–2976, Aug. 2005.
- [54] D. Love and R. Heath. Limited feedback diversity techniques for correlated channels. *IEEE Trans. Veh. Technol.*, 55(2):718–722, Mar. 2006.
- [55] D. Love, R. Heath, V. Lau, D. Gesbert, B. Rao, and M. Andrews. An overview of limited feedback in wireless communication systems. *IEEE J. Sel. Areas Commun.*, 26(8):1341–1365, Oct. 2008.
- [56] D. Love, H. R.W., and T. Strohmer. Grassmannian beamforming for multiple-input multiple-output wireless systems. *IEEE Trans. Inf. Theory*, 49(10):2735–2747, Oct. 2003.
- [57] H. Määttänen, K. Schober, O. Tirkkonen, and R. Wichman. Precoder partitioning in closed-loop MIMO systems. *IEEE Trans. Wireless Commun.*, 8(8):3910–3914, Aug. 2009.
- [58] B. Mondal, S. Dutta, and R. Heath. Quantization on the Grassmann manifold. *IEEE Trans. Signal Process.*, 55(8):4208–4216, Aug. 2007.
- [59] B. Mondal and R. Heath. Performance analysis of quantized beamforming MIMO systems. *IEEE Trans. Signal Process.*, 54(12):4753–4766, Dec. 2006.
- [60] B. Mondal, T. Thomas, and M. Harrison. Rank-independent codebook design from a quaternary alphabet. In *Proc. Asilomar Conf. on Signals, Systems and Computers*, pages 297–301, Nov. 2007.
- [61] K. K. Mukkavilli, A. Sabharwal, E. Erkip, and B. Aazhang. On beamforming with finite rate feedback in multiple-antenna systems. *IEEE Trans. Inf. Theory*, 49(10):2562–2579, Oct. 2003.
- [62] S. Murray and C. Sämann. Quantization of flag manifolds and their supersymmetric extensions. *Adv. Theor. Math. Phys.*, 12(3):641–710, 2008.
- [63] C. Murthy and B. D. Rao. Quantization methods for equal gain transmission with finite rate feedback. *IEEE Trans. Sig. Proc.*, 55(1):233–245, Jan. 2007.
- [64] A. Narula, M. Lopez, M. Trott, and G. Wornell. Efficient use of side information in multiple-antenna data transmission over fading channels. *IEEE J. Sel. Areas Commun.*, 16(8):1423–1436, Oct. 1998.

- [65] J. Nash. C1 isometric imbeddings. *Ann. Math. (2)*, 60(3):383–396, Nov. 1954.
- [66] F. Oggier. A survey of algebraic unitary codes. In *Coding and Cryptology*, pages 171–187. Springer, 2009.
- [67] J. Oprea. *Differential Geometry and Its Applications*. Prentice Hall, 2003.
- [68] R. Picken. The Duistermaat-Heckman integration formula on flag manifolds. *J. of Math. Phys.*, 31(3):616–638, Mar. 1990.
- [69] R.-A. Pitaval, H.-L. Määttänen, K. Schober, O. Tirkkonen, and R. Wichman. Beamforming codebooks for two transmit antenna systems based on optimum grassmannian packings. *IEEE Trans. Inf. Theory*, 57(10):6591–6602, Oct. 2011.
- [70] R. Rankin. The closest packing of spherical caps in n dimensions. *Proc. Glasgow Math. Assoc.*, 2:139–144, 1955.
- [71] J. Roh and B. Rao. Design and analysis of MIMO spatial multiplexing systems with quantized feedback. *IEEE Trans. Sig. Proc.*, 54(8):2874–2886, Aug. 2006.
- [72] J. Roh and B. Rao. Transmit beamforming in multiple-antenna systems with finite rate feedback: a VQ-based approach. *IEEE Trans. Inf. Theory*, 52(3):1101–1112, Mar. 2006.
- [73] A. Roy. Bounds for codes and designs in complex subspaces. *J. Algebraic Combin.*, 31(1):1–32, 2010.
- [74] E. Saff and A. Kuijlaars. Distributing many points on a sphere. *Math. Intell.*, 19(1):5–11, 1997.
- [75] J. Saltz. Digital transmission over cross-coupled linear channels. *AT & T Technical Journal*, 64(6):1147–1159, July-Aug. 1985.
- [76] K. Schober, P. Janis, and R. Wichman. Geodesical codebook design for pre-coded mimo systems. *IEEE Commun. Lett.*, 13(10):773–775, Oct. 2009.
- [77] E. Sengul, H. Park, and E. Ayanoglu. Bit-interleaved coded multiple beamforming with imperfect CSIT. *IEEE Trans. Commun.*, 57(5):1505–1513, May 2009.
- [78] A. Shokrollahi, B. Hassibi, B. Hochwald, and W. Sweldens. Representation theory for high-rate multiple-antenna code design. *IEEE Trans. Inf. Theory*, 47(6):2335–2367, 2001.
- [79] P. Shor and N. J. Sloane. A family of optimal packings in Grassmannian manifolds. *J. Algebraic Combin.*, 7:157–163, 1998.
- [80] T. Shuang, T. Koivisto, H.-L. Maattanen, K. Pietikainen, T. Roman, and M. Enescu. Design and evaluation of LTE-Advanced double codebook. In *Proc. IEEE Veh. Technol. Conf.*, pages 1–5, May 2011.
- [81] V. Sidelnikov. On a finite group of matrices generating orbit codes on Euclidean sphere. In *Proc. IEEE Int. Symp. Inf. Theory*, page 436, June 1997.
- [82] D. Slepian. Group codes for the Gaussian channel. *Bell Syst. Techn. J.*, 47(4):575–602, Apr. 1968.



- [83] N. Sloane. Neil J. A. Sloane: Home page. published electronically at <http://www.research.att.com/~njas/index.html#TABLES>.
- [84] N. Sloane, with the collaboration of R.H. Hardin, W. Smith, et al. Tables of spherical codes. published electronically at [www.research.att.com/~njas/packings/](http://www.research.att.com/~njas/packings/).
- [85] T. Strohmer and R. Heath. Grassmannian frames with applications to coding and communication. *Appl. Comput. Harmon. A.*, 14(3):257–275, 2003.
- [86] D. Su, X. Hou, and C. Yang. Quantization based on per-cell codebook in cooperative multi-cell systems. In *Proc. IEEE Wireless Commun. & Net. Conf.*, pages 1753–1758, Mar. 2011.
- [87] E. Telatar. Capacity of multi-antenna gaussian channels. *Eur. T. Telecommun.*, 10:585–595, 1999.
- [88] L. Thiele, M. Schellmann, T. Wirth, and V. Jungnickel. Cooperative multi-user MIMO based on limited feedback in downlink OFDM systems. In *Proc. Asilomar Conf. on Signals, Systems and Computers*, pages 2063–2067, Oct. 2008.
- [89] E. Visotsky and U. Madhow. Space-time transmit precoding with imperfect feedback. *IEEE Trans. Inf. Theory*, 47(6):2632–2639, Sep. 2001.
- [90] S. Wagner, S. Sesia, and D. Slock. Unitary beamforming under constant modulus constraint in MIMO broadcast channels. In *Proc. IEEE Workshop Sig. Process. Adv. Wireless Commun.*, pages 151–155, June 2009.
- [91] S. Wagner, S. Sesia, and D. Slock. On unitary beamforming for MIMO broadcast channels. In *Proc. IEEE Int. Conf. Commun.*, pages 1–5, May 2010.
- [92] L. Whyte. Unique arrangements of points on a sphere. *Amer. Math. Monthly*, 59:606–611, 1952.
- [93] R. Wichman and A. Hottinen. Transmit diversity in the WCDMA system. *Int. J. Wireless Inf. Networks*, 6:171–180, 1999.
- [94] P. Xia. *Multi-Input Multi-Output Communications with Partial Channel State Information*. PhD thesis, University of Minnesota, 2005.
- [95] P. Xia and G. Giannakis. Design and analysis of transmit-beamforming based on limited-rate feedback. *IEEE Transactions on Signal Processing*, 54(5):1853–1863, May 2006.
- [96] P. Xia, S. Zhou, and G. Giannakis. Achieving the Welch bound with difference sets. *IEEE Trans. Inf. Theory*, 51(5):1900–1907, May 2005.
- [97] L. Zheng and D. Tse. Communication on the Grassmann manifold: a geometric approach to the noncoherent multiple-antenna channel. *IEEE Trans. Inf. Theory*, 48(2):359–383, Feb. 2002.
- [98] K. Zyczkowski and H.-J. Sommers. Hilbert-Schmidt volume of the set of mixed quantum states. *J. Phys. A: Math. Gen.*, 36(39):10115–10130, 2003.

# Errata

## Publication I

p. 2299, first paragraph, the principal angles are given by the SVD of  $Y^\dagger Z$  not  $YZ^\dagger$ .

## Publication III

The symbol of the border of the spherical cap  $\mathcal{C}_i(z)$  did not print correctly, as a result both the cap and its border are defined by  $C_i(z)$ :

- p. 6597, the last equation should be:

$$\mathcal{C}_i(z) = \{\mathbf{y} \in S^2(\frac{1}{2}) : |\mathbf{y} - \mathbf{x}_i|^2 = z\}.$$

- p. 6598, the derivation of equation (24) should read:

$$\begin{aligned} \mathcal{A}(C_i(z) \cap V_i) &= \iint_{C_i(z) \cap V_i} \frac{1}{2} d\mathbf{j} d\phi_i \\ &= \int_0^z \left( \frac{1}{2} \int_{\mathcal{C}_i(\mathbf{j}) \cap V_i} d\phi_i \right) d\mathbf{j}. \end{aligned}$$

The pdf of the squared distance  $f_{d_c^2}$  is then obtained by straightforward differentiation:

$$\frac{d}{dz} (\mathcal{A}(C_i(z) \cap V_i)) = \frac{1}{2} \int_{\mathcal{C}_i(z) \cap V_i} d\phi_i,$$

and finally we have

$$f_{d_c^2}(z) = \frac{1}{2\pi} \sum_{i=1}^N \int_{\mathcal{C}_i(z) \cap V_i} d\phi_i.$$

The integral in the last equality can be calculated by taking into account the fact that the discontinuities of  $\mathcal{C}_i(z) \cap V_i$  belong to the borders of  $V_i$ .

#### Publication IV

- p. 5 Table III, the entries of some codewords are incorrect. A corrected version is given in Table 5.4.
- p. 3 Proposition 2, and p. 4 Proposition 4, *totally singular subspaces* should be understood as *totally isotropic subspaces*. Singular and isotropic subspaces was the terminology used in [14] when considering vector spaces over the field of integers modulo 2 and 4, leading to real and complex packings, respectively.
- p. 3, last line, the normalization  $\{1/\sqrt{2}A\}$  is incorrect, the factor  $1/\sqrt{2}$  apply only to the last four codewords of A and not the first two ones.

#### Publication VIII

- Selection of codewords is not clearly specified in the paper, we provide details here:
  - In Fig. 1, as we were comparing coding in different manifolds, the codeword selection was performed using the optimal selection that correspond to maximize the information rate. It follows that the statement p. 5 “When using this scheme, we have selected the codeword minimizing the flag distance  $d_p$  over all combinations of Grassmannian and orthogonalization codewords.” is erroneous.
  - In Fig. 2, the codewords selection was performed with the permutation-invariant flag chordal distance  $d_p$ .
- Additionally, there are typos on the labelling of Fig. 2: for  $N_t = 4$ , the curves corresponds to 1, 2, 3, and 5 feedback bits.







ISBN 978-952-60-5491-9  
ISBN 978-952-60-5492-6 (pdf)  
ISSN-L 1799-4934  
ISSN 1799-4934  
ISSN 1799-4942 (pdf)

**Aalto University**  
**School of Electrical Engineering**  
**Department of Communications and Networking**  
[www.aalto.fi](http://www.aalto.fi)

**BUSINESS +  
ECONOMY**

**ART +  
DESIGN +  
ARCHITECTURE**

**SCIENCE +  
TECHNOLOGY**

**CROSSOVER**

**DOCTORAL  
DISSERTATIONS**